Term Project Final Report

Author: Dominic Riccoboni

Course: EE514 - Advanced Topics in Automatic Control

To: Dr. Clay McKell

Table of Contents

Part One - Modelling, Early Lyapunov Stability Analysis, and Linear Quadratic Regulator Design

Modelling

Determining System Parameters from Experimental Data

First, the experimental data is imported and the values of system constants K_m, K_t, K_p, and K_a are determined using various techniques. The data is found in the "SS_speeds_voltages_data.xlsx" excel spreadsheet located in the "Exp Data" repository sub-folder. The constants are defined:

$$K_m = \frac{\omega_{ss}}{v_m}$$

$$K_t = \frac{v_t}{\omega}$$

$$K_p = \frac{v_p}{\theta_o}$$

$$K_a = \frac{v_m}{v_o}$$

K_m is the motor speed constant (which is related to additional motor parameters below), the tachometer constant is K_t, the potentiometer constant is K_p, and the inverting power amplifier constant is K_a. The variable ω_{ss} is the motor's steady state angular velocity reached when a step input voltage of v_m is applied. The voltage v_t is an output of the tachometer for any given instantaneous motor angular velocity ω. For the position constant, the voltage v_p represents the potentiometer voltage reading given gear reduced ouput angle θ_o. This output angle is related to the motor shaft angle through gear ratio N:

$$\theta_o = \frac{\theta_m}{N}.$$

In addition to these parameters, the motor-with-gearbox open loop time constant τ_m must be determined from step response data provided. This, along with K_m (also determined experimentally) will provide for almost all of the relationships that will be needed to model the motor within the system. Their equations are:

$$\tau_m = \frac{J_m}{K_{fm} + \frac{K_c}{R_a} K_b}$$

and

$$K_m = \frac{\frac{K_c}{R_a}}{K_{fm} + \frac{K_c}{R_a} K_b}$$

Where K_{fm} is the motor's viscous damping coefficient, R_a is its armature resistance, K_c is its torque/current constant, K_b is its back emf constant, and J_m is the combined mass moment of inertia of the motor armature and the gearbox. One more experimental measurement is required - the ratio $\dfrac{K_c}{R_a}$ can be ascertained from the static torque required to move the pendulum from equilibrium when it is at -90 degrees (horizontal). This static torque-voltage constant is found from:

$$\frac{K_c}{R_a} = \frac{MgL}{v_{m,0}}$$

where M is the mass of the pendulum bob, g is the gravitational constant, and L is the moment arm from the pendulum's point of rotation to the pendulum bob.

Motor Speed Constant and the Breakaway Voltage

K_m is determined from the slope of a linear curve fit to the non-zero data points.

```
Km is found to be 220.9 [RPM/V]
```

Breakaway voltage, v_{ba}, is determined by finding x intercept of the linear curve fit to all non-zero voltage data points.

```
Breakaway voltage is found to be 1.0684 [V]
```

3

Steady State Motor Speed vs Armature Voltage Plot

$K_m = 220.9$[RPM/V]

Breakaway Voltage = 1.0684[V]
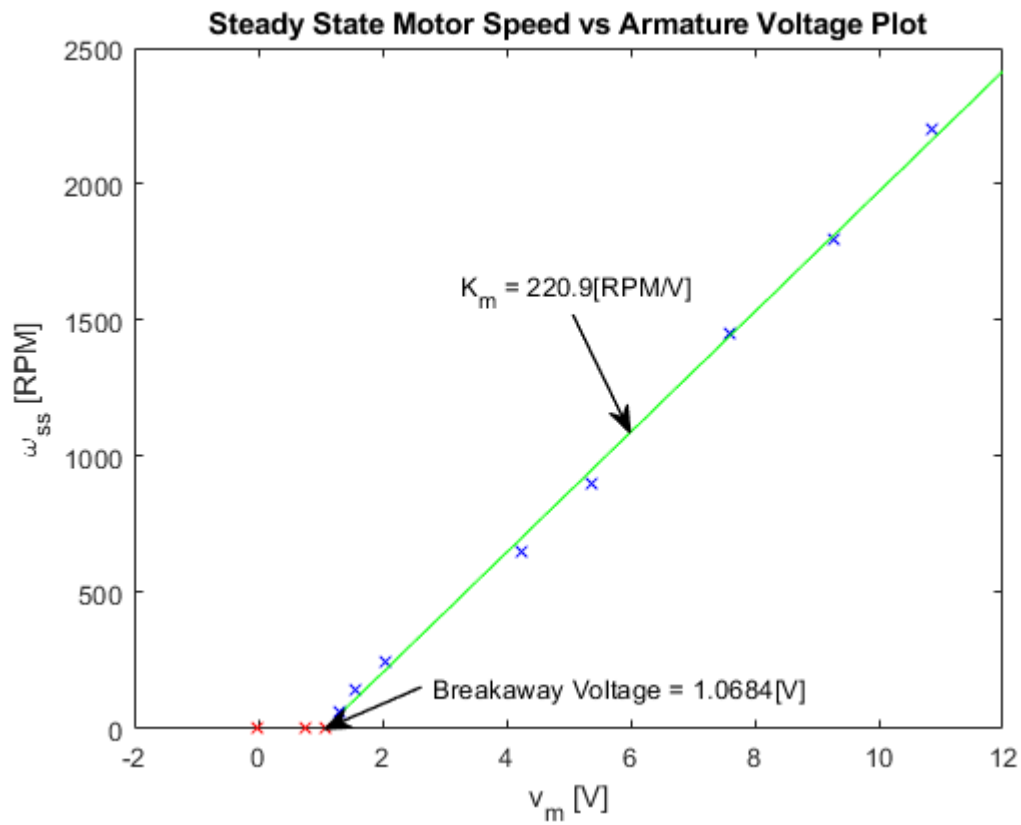
Tachometer Constant

A linear curve fit is used to approximate the tachometer measurement constant $K_t = \dfrac{v_t}{\omega}$ from experimental data.

```
Kt is found to be -0.015 [V/RPM]
```

Motor Speed vs Tachometer Voltage Reading

$K_t = -0.015[V/RPM]$
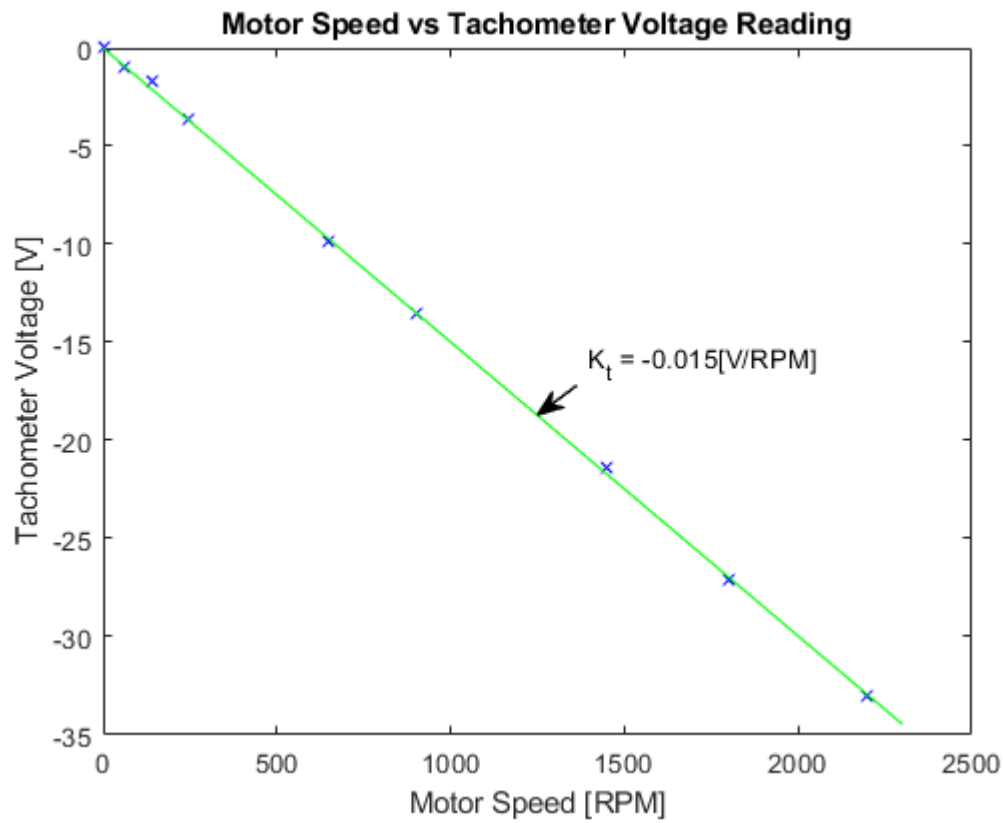
Inverting Power Amplifier Constant

A linear curve fit is used to approximate the tachometer measurement constant $K_a = \dfrac{v_m}{v_o}$ from experimental data.

```
Ka is found to be -5.0204 [V/V]
```

Armature Voltage vs Op Amp Voltage

$K_a = -5.02[V/V]$

Motor Voltage, v_m [V] (vertical axis)

Inverting Op Amp Output Voltage v_o [V] (horizontal axis)
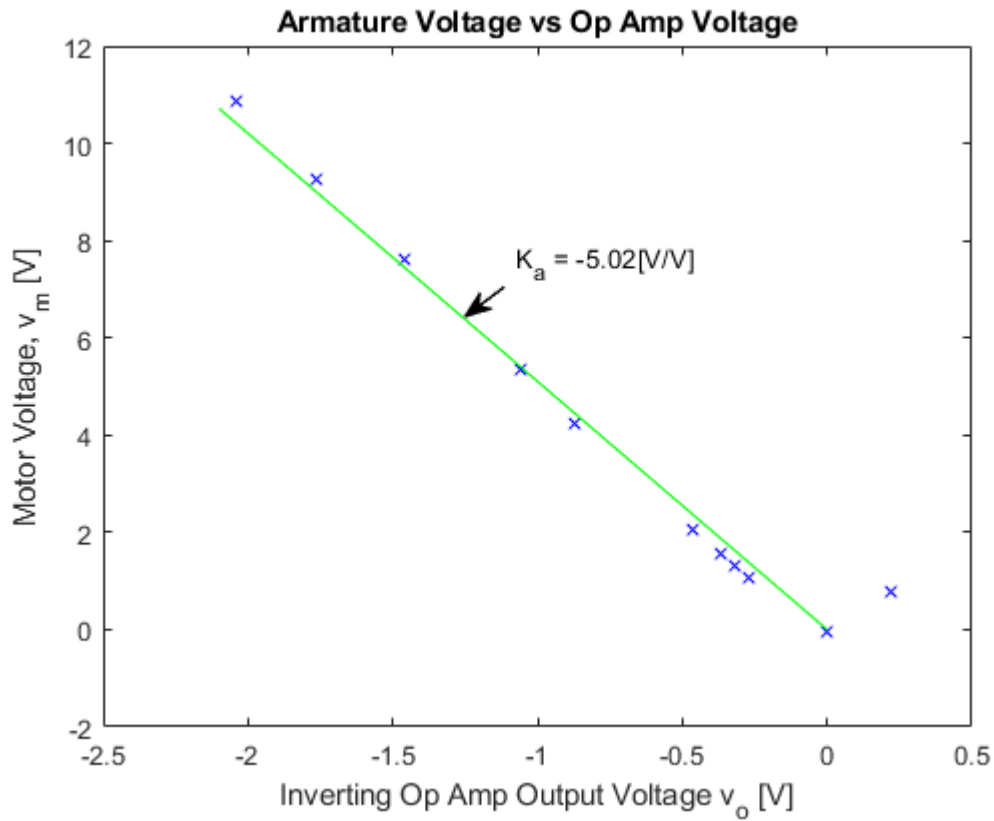
Potentiometer Constant

Data is separated (roughly) by linear regions of the sawtooth wave and a linear curve fit is given to each. The slopes are then averaged to determine a value in volts per second.

```
First slope fit is 52.207 [V/s]
Second slope fit is 52.496 [V/s]
Third slope fit is 52.6473 [V/s]
```

Potentiometer Voltage vs Time
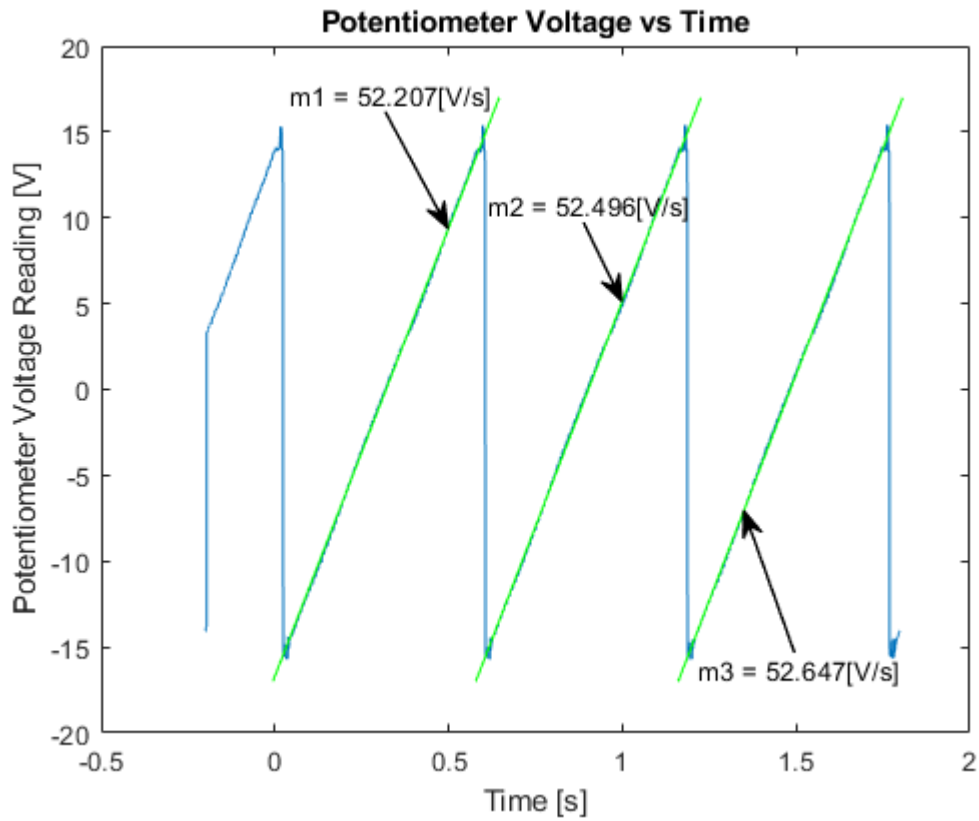
The period of the sawtooth waveform is found by manually finding the timespan associated with the initial and final positive peak of the data and dividing that by three.

Using the average of the slopes determined from the three linear curve fits above, K_p is computed.

$$K_p = \frac{2\pi * avg(m_1, \ m_2, \ m_3)}{T_p}$$

Potentiometer Voltage vs Time

X 1.763
Y 15.4133

Potentiometer Voltage vs Time

X 0.016
Y 15.2957
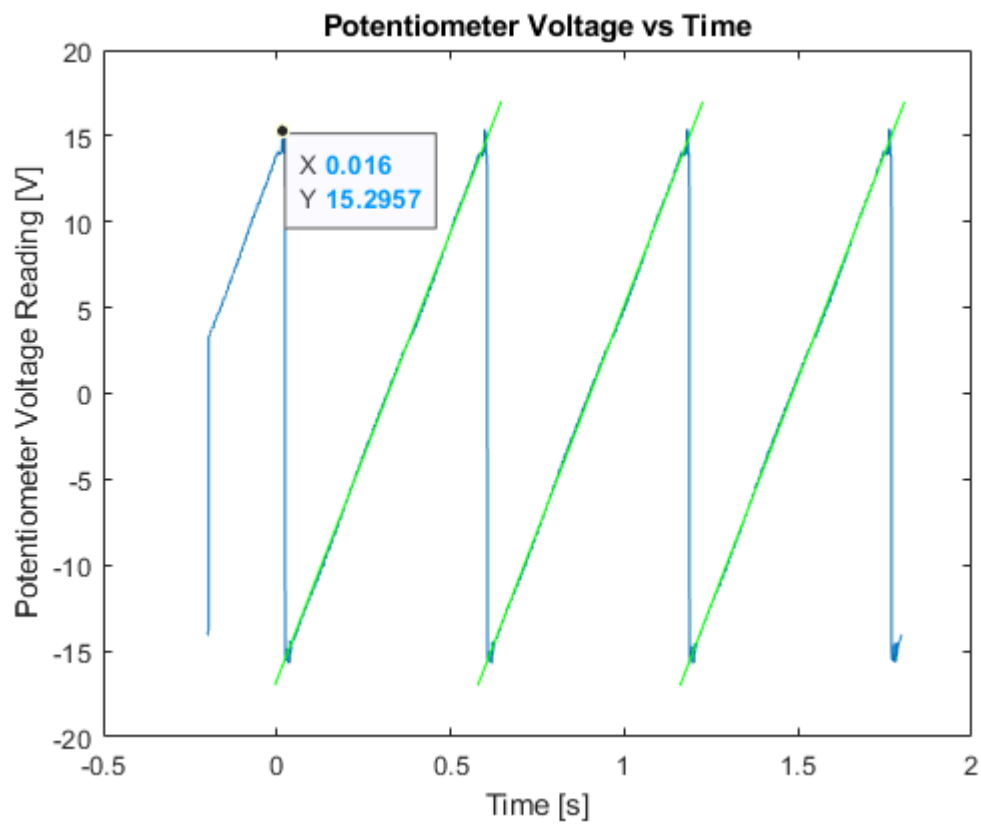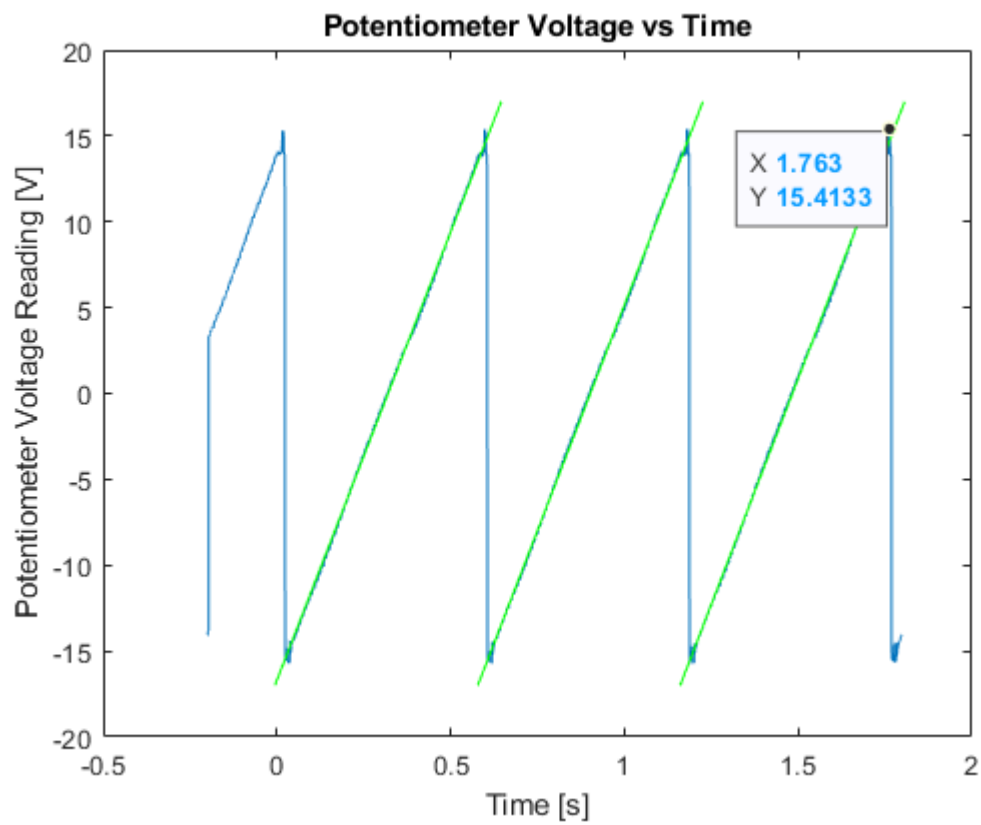
T_p is found to be 0.582 [sec]

K_p is found to be -4.9 [V/rad]

Motor Time Constant

First, an estimate of the steady state voltage is found by averaging a range of values near the end of the data collected for each step response. The final one percent of the data points are used for each calculation.

```
Steady state tachometer reading 1 is found to be 23.364 [Volts]

Steady state tachometer reading 2 is found to be 25.031 [Volts]

Steady state tachometer reading 3 is found to be 14.092 [Volts]
```

To better estimate the time constant, a 100 point moving mean is used to attempt to smooth out the data in the transient regions. This is shown in red and overlays the raw data plotted below.

Next, the first voltage to exceed 63.21% of the step response's steady state voltage is found from the *averaged* data, not the raw data. Its associated time is taken to be the time constant for the response.

```
Time constant for step response 1 is found to be 0.28634 [s]

Time constant for step response 2 is found to be 0.27293 [s]

Time constant for step response 3 is found to be 0.25984 [s]
```

Finally, the motor's time constant is taken to be the average of these three values

```
The motor time constant is found to be 0.273 [s]
```

Finally, results are plotted with raw data, smoothed data, steady state voltage value, and associated time constants overlayed.

Plot of Step Response 1:

$V_{t,ss} = 23.364 [V]$

$\tau_1 = 0.286 [s]$ at a value of $14.9 [V]$

Plot of Step Response 2:

$V_{t,ss} = 25.031 [V]$

$\tau_2 = 0.273 [s]$ at a value of $16 [V]$
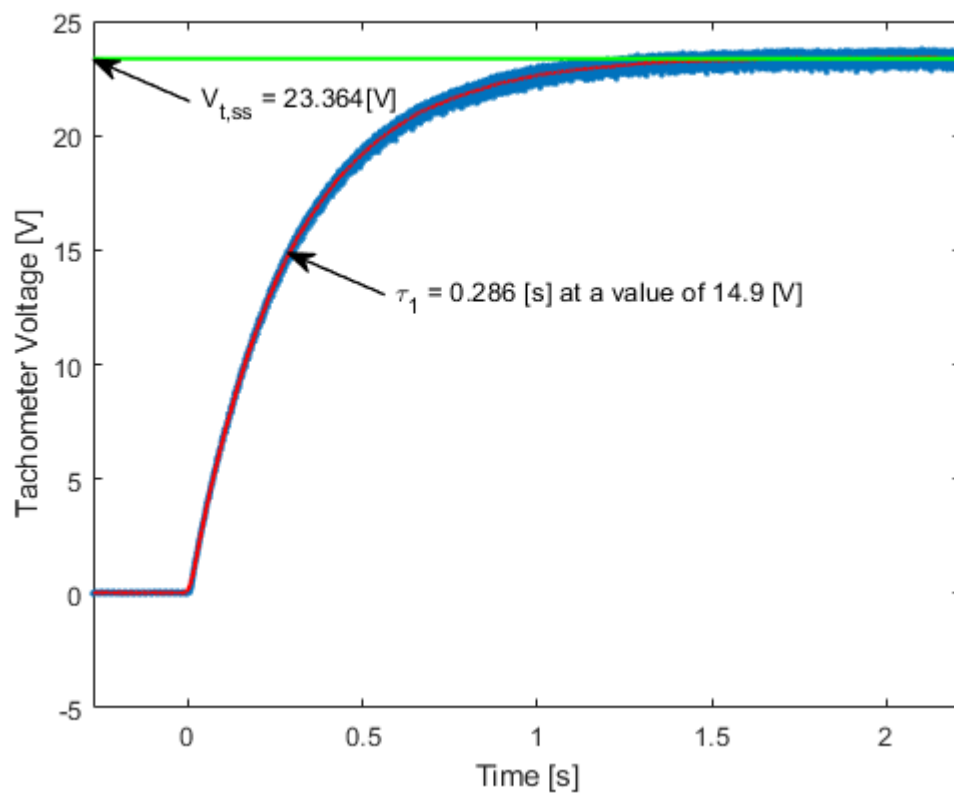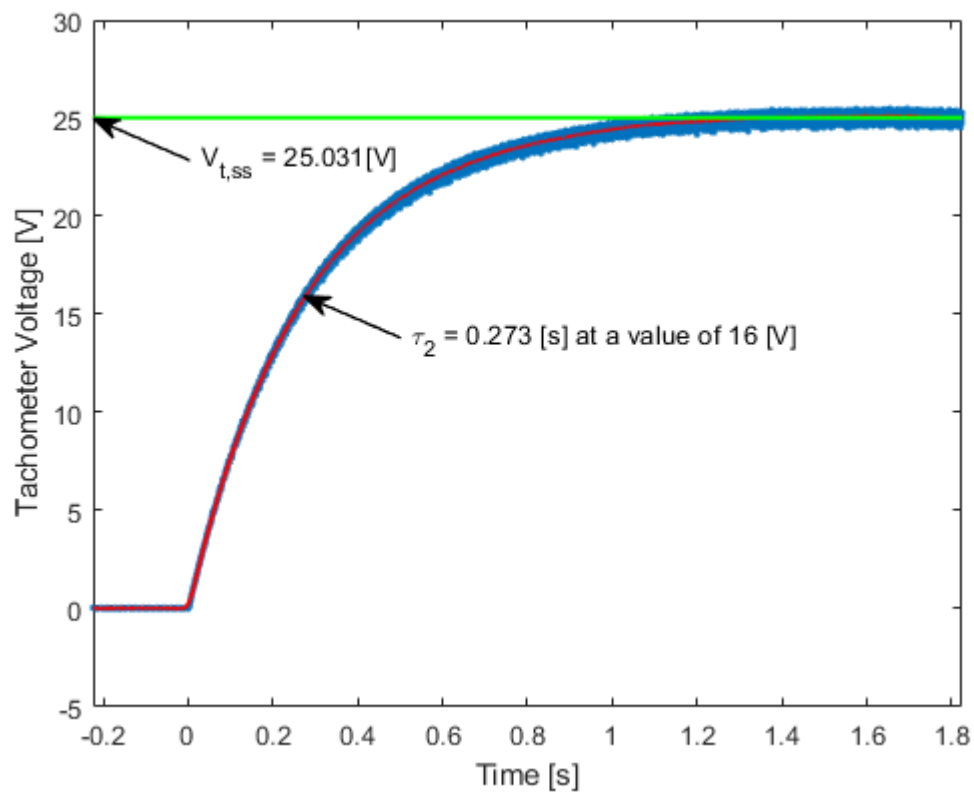
Plot of Step Response 3:
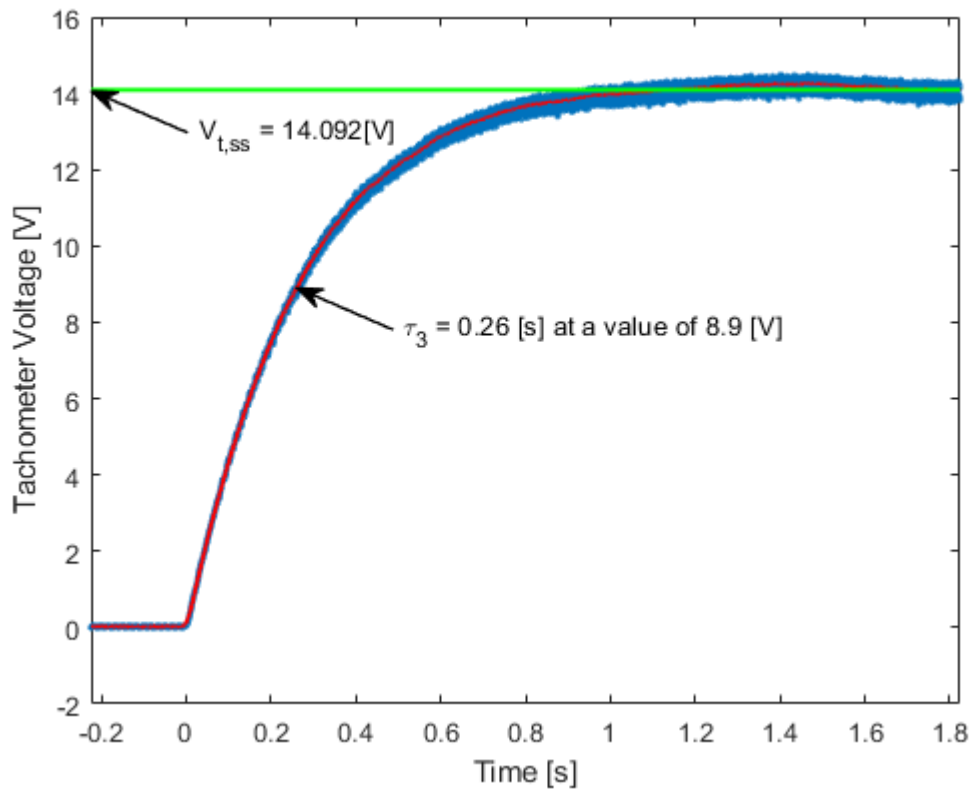
Static Torque Voltage Constant $\dfrac{K_c}{R_a}$

$$\frac{K_c}{R_a} = \frac{MgL}{v_{m,0}}$$

Where

$$M = 0.028 \ [kg]$$

$$L = 0.0254 \ [m]$$

$$g = 9.81 \ \left[\frac{m}{s^2}\right]$$

$$v_{m,0} = 0.66 \ [V]$$

The static torque voltage constant is found to be 0.1163 [Nm/V]

Torque Required to Break Through the Static Friction in the Step Responses

The motor circuit is modelled in the following manner.
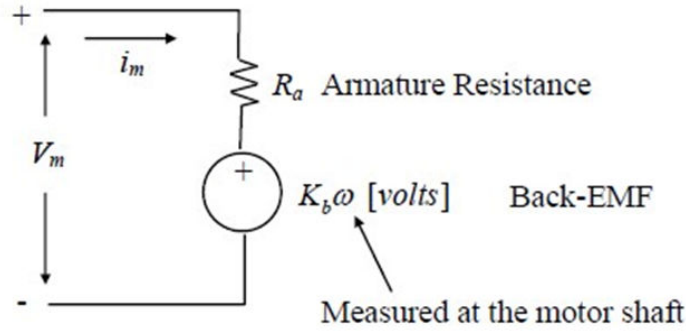
In the static friction case, when the motor is stalled, no ω has developed in the system and all the electrical power is being dissipated as heat through R_a. The armature KVL in this scenario is

$$v_m = i_m R_a$$

The torque produced by a DC motor is given by

$$T_m = K_c i_m$$

Therefore,

$$T_m = \frac{K_c}{R_a} v_m$$

The torque required to break the system out stall, T_{ba}, is related to the breakaway voltage, v_{ba}, from the ω_{ss} vs v_a dataset through the stalled motor condition. At the tipping point

12

$$T_{ba} = \frac{K_c}{R_a} v_{ba}$$

There is an inherent assumption here that most of the static friction torque is lumped at the motor side of the speed reducer, not the pendulum side. In reality, there is a contribution to stiction from the individual mechanical elements of the reducer. Since it would be out of the scope of this report to determine what exactly is contributing to stiction and its consequence on the static force balance problem, this is an assumption that must be made.

```
The breakaway torque is found to be 0.1242 [Nm]
```

Algebraically Determining the Remaining System Parameters

First, convert constants to SI units

```
The motor velocity constant Km is 23.133 [rad/Vs]
The tachometer constant Kt is -0.143 [Vs/rad]
```

The friction constant K_{fm} and back emf constant K_b are common to both τ_m and K_m and can be eliminated. This allows us to solve for the motor inertia in terms of other known constants.

$$J_m = \frac{K_c \, \tau_m}{R_a \, K_m}$$

```
The motor polor moment of inertia Jm is 0.0014 [kg-m-s^2]
```

Relating Found System Parameters to a Nonlinear Motorized Pendulum Model

A schematic representation of the motorized pendulum system is shown below.
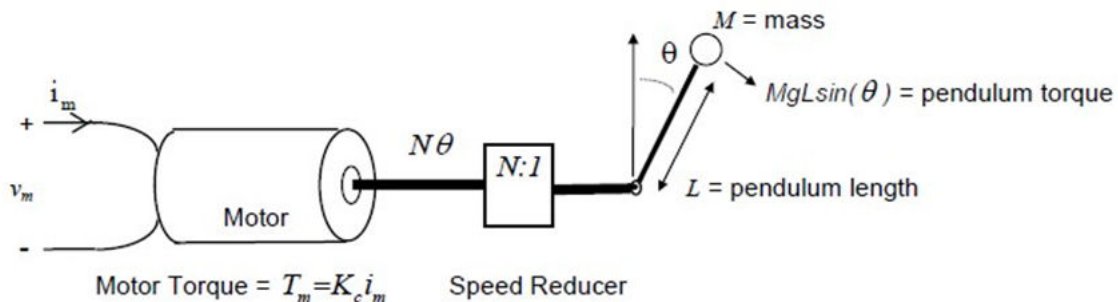
A nonlinear model of the pendulum kinetics is expressed in terms of an input armature voltage actuation as such:

$$\frac{K_c}{R_a}v_m = \dot{\theta}\left(K_{fm}N + \frac{K_b K_c N}{R_a}\right) + \ddot{\theta}(J_m N + J_p) - LMg\sin(\theta)$$

Where friction due to the pendulum itself is assumed to be negligible. The pendulum's moment of inertia, J_p, is given by

$$J_p = L^2 M$$

and $N = 8.1$ is a gear ratio between the motor shaft and the pendulum. The input to the system is voltage v_m, the motor's armature voltage - this can be related to our control actuation v_o through K_a. This will have to be done for all of the measured states as well so that gain selecting resistors can be placed in the electronics. From rearranging the equation for τ_m, the terms $K_{fm} + K_b\frac{K_c}{R_a}$ in the pendulum model can be eliminated in favor of known values.

$$\tau_m = \frac{J_m}{K_{fm} + \frac{K_c}{R_a}K_b}$$

$$\frac{\tau_m}{J_m} = \frac{1}{K_{fm} + \frac{K_c}{R_a}K_b}$$

$$K_{fm} + K_b\frac{K_c}{R_a} = \frac{J_m}{\tau_m}$$

And from J_m above

$$K_{fm} + K_b \frac{K_c}{R_a} = \frac{1}{K_m} \frac{K_c}{R_a}$$

Hence

$$\frac{K_c v_m}{R_a} = \ddot{\theta}(J_m N + J_p) - L M g \sin(\theta) + \frac{K_c N \dot{\theta}}{K_m R_a}$$

The above model excludes any modelling of additional nonlinearities in the system. The model will be supplemented with a coulomb friction with damping nonlinearity. This replaces the $\dfrac{K_c N}{K_m R_a}$ damping coefficient in the above model. This damping coefficient is captured by the nonlinear friction model in the slope of the linear regions of the T_f vs $\dot{\theta}$ plot below. Its offset is the breakaway torque required to overcome the stiction. The signum function inherent in this model will act as a switching law around zero pendulum/motor velocity that tends the system back to zero velocity if the net torques on the armature to not exceed a threshold.
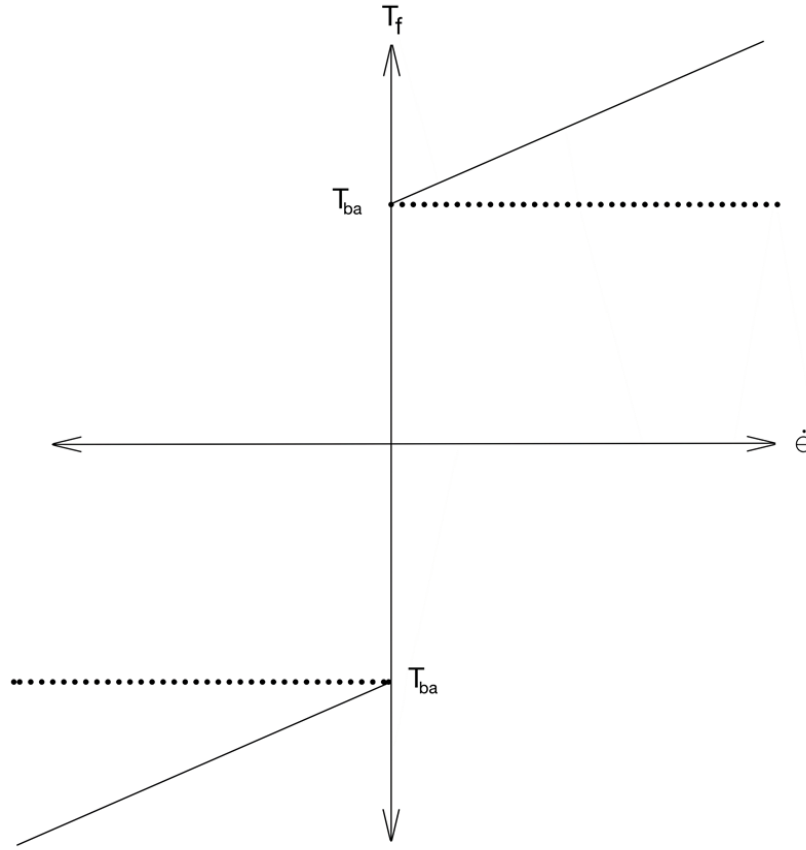
The analytical expression for the friction term T_f is

$$T_f \;=\; |T_{ba}| sign(\dot{\theta}) \;+\; \frac{K_c N}{K_m R_a} \dot{\theta}$$

and the pendulum EOM becomes

$$\frac{K_c v_m}{R_a} \;=\; \ddot{\theta}\,(J_m N + J_p) - L\,M\,g\,\sin(\theta) + |T_{ba}| sign(\dot{\theta}) \;+\; \frac{K_c N}{K_m R_a} \dot{\theta}$$

Summary of Numerical Constants

This table summarizes the minimum number of constants, determined from experimental data, needed to implement the full nonlinear pendulum model in Simulink.

Constant	Value
$K_m \; [\frac{rad}{s}/V]$	23.13
$K_t \; [V/\frac{rad}{s}]$	−0.143
$K_p \; [\frac{V}{rad}]$	−4.86
$K_a \; [\frac{V}{V}]$	−5.02
$\tau_m \; [s]$	0.2730
$J_m \; [kgms^2]$	0.0014
$N \; [\frac{rad}{rad}]$	8.1
$J_p \; [kgms^2]$	0.0022
$T_{ba} \; [Nm]$	0.1242
$V_{ba} \; [V]$	1.0684
$\frac{K_c}{R_a} \; [\frac{Nm}{V}]$	0.1163

Nonlinear State Space Representation of the Motorized Pendulum

The nonlinear state space representation *excluding the stiction nonlinearity* is

$$\dot{\vec{x}} = f(\vec{x}, v_m)$$

where $\vec{x} = [\theta \; \dot{\theta}]^T$. Hence,

$$\begin{bmatrix} \dot{\theta} \\ \ddot{\theta} \end{bmatrix} = \begin{bmatrix} \dot{\theta} \\ \dfrac{K_c v_m}{J_m N R_a + J_p R_a} - \dfrac{K_c N \dot{\theta}}{J_m K_m N R_a + J_p K_m R_a} + \dfrac{L M g \sin(\theta)}{J_m N + J_p} \end{bmatrix}$$

Taking the Jacobian with respect to the state yields

$$J_x(\vec{x}) = \begin{bmatrix} 0 & 1 \\ \dfrac{L\,M\,g\cos(\theta)}{J_m N + J_p} & -\dfrac{K_c N}{J_m K_m N R_a + J_p K_m R_a} \end{bmatrix}$$

and the Jacobian with respect to the input is simply a linear input matrix B

$$J_u = B = \begin{bmatrix} 0 \\ \dfrac{K_c}{J_m N R_a + J_p R_a} \end{bmatrix}$$

Stability Analysis

It is clear from the $f(\vec{x}, v_m)$ that the open loop ($v_m = 0$) equilibrium points are located at $\dot{\theta} = 0$, and $\sin(\theta) = 0$. So, for θ at integer multiples of π, the pendulum is naturally stable when $\dot{\theta}$ is zero. It is also possible to consider the actuated equilibrium points, ones where v_m is compensating for gravity at an arbitrary pendulum angle. One can imagine designing a feed-forward control law around those points where feed forward voltage $v_{m,ff}$ creates an equilibrium point at some nonzero θ_{eq}. A regulator around error states in position and velocity can then be analyzed for stability. There are likely many ways to consider stability in the actuated case, all depending on the control law utilized. This paper will focus on stability analysis of the natural equilibrium points as well as a closed loop stability analysis of the operating point at $\theta = 0$.

The two natural equilibrium points will be analyzed for open loop stability. The upward position, $\theta = 0$, will be shown asymptotically unstable using Lyapunov's indirect method. The downward position, $\theta = \pi$, will be shown asymptotically stable using the same method. A stabilizing linear quadratic regulator will be designed about the upward operating point. Again, Lyapunov's indirect method will be used to argue for asymptotic stability of the closed loop system.

Natural Equilibrium Points

Since $\vec{x_d} = (\theta_d, \dot{\theta}_d) = (0,0)$ is an equilibrium point, it is valid to use Lyapunov's indirect method to make a statement about the asymptotic stability of the point. Eigenvalue analysis of the system's Jacobian evaluated at that point tells us if the point is asymptotically stable or unstable. The Jacobian here will be denoted A_1

$$A_1 = \begin{bmatrix} 0 & 1 \\ 5.7692 & -3.0608 \end{bmatrix}$$

The eigenvalues of this matrix are

$$\begin{bmatrix} \lambda_1 \\ \lambda_2 \end{bmatrix} = \begin{bmatrix} -4.3784 \\ 1.3177 \end{bmatrix}$$

Since one of the eigenvalues is positive real, the point is asymptotically unstable.

The point $\vec{x_d} = (\pi, 0)$ is also an equilibrium point. Its Jacobian is A_2

$$A_2 = \begin{bmatrix} 0 & 1 \\ -5.7692 & -3.0608 \end{bmatrix}$$

The eigenvalues of this matrix are

$$\begin{bmatrix} \lambda_1 \\ \lambda_2 \end{bmatrix} = \begin{bmatrix} -1.5304 - 1.8513\,\mathrm{i} \\ -1.5304 + 1.8513\,\mathrm{i} \end{bmatrix}$$

Since neither of these have a positive real part, the point is asymptotically stable.

Stability of a Linear Quadratic Regulator About Upward Position

For an actuated system, the linearization necessary for Lyapunov's indirect method must include a nominal value of the actuation.

$$f(\vec{x}, v_m) \approx f(\vec{x_d}, v_{m,d}) + J_x(\vec{x_d}, v_{m,d})\delta \vec{x} + J_u(\vec{x_d}, v_{m,d})\delta v_m$$

where

19

$$\delta \vec{x} = \vec{x}_d - \vec{x}$$

and

$$\delta v_m = v_{m,d} - v_m$$

Since the system is naturally stable at the operating point, if $v_m = -K\vec{x}$ where $K = [K_1 \ K_2]^T$, then

$$v_{m,d} = -K\vec{x}_d = \vec{0}$$

and

$$\delta v_m = v_m$$

Therefore, a full state feedback law in absolute actuation is possible. A change of variables to deviation states will not be necessary to implement the linear controller. The linearized system with full state feedback has the closed loop matrix $A'_1 = A_1 - BK$. If a K matrix is chosen such that the eigenvalues of A'_1 have negative real part, then the equilibrium point will be closed loop asymptotically stable. Since solutions to the linear quadratic regulator problem are guaranteed to produce stable eigenvalues in the closed loop matrix, our system will be asymptotically stable at the upward operating point. This will prove to be insufficient for good control, however. It only guarantees that there is *some* region in the state space for which trajectories that begin within that region will asymptotically approach the operating point. If it is desired to obtain information about the size of this region, additional Lyapunov techniques would be necessary. These alternatives will not be explored in this paper. Below is the linearized system for the LQR controller.

$$f(\vec{x}, v_m) \approx J_x(\vec{0})\vec{x} + J_u(-K\vec{x})$$

i.e.

$$\dot{\vec{x}} \approx A_1 \vec{x} - BK \vec{x}$$

$$\dot{\vec{x}} \approx (A_1 - BK) \vec{x}$$

$$\dot{\vec{x}} \approx A'_1 \vec{x}$$

This stability analysis has not considered the nonlinear stiction present in the system. This could prove to be a problem for some controllers as high stiction could cause integrator windup, steady state error affecting the asymptotic nature of the equilibrium points, or some other type of effect. This analysis will only consider the stiction through simulation.

Simulated Step Responses of the System with Stiction and no Pendulum

This shows that the modelled system, with stiction, reproduces the steady state velocity vs armature voltage relationship - that the K_m and V_{ba} values computed from raw data are represented in the model. Below is a plot of the raw data, original curve fit, and a set of steady state values from simulation step responses. The K_m value was utilized in the model along with the other constants determined above and the stiction nonlinearity. The K_m curve fit and the simulated data line up so perfectly that one set is hidden by the other. This is an indicator that, at the very least, the parameters found from experimental data are consistent with each other and with the model. It also indicates that significant elements of the raw data are represented by the simulation utilized in the control system design.

Steady State Motor Speed vs Armature Voltage Plot
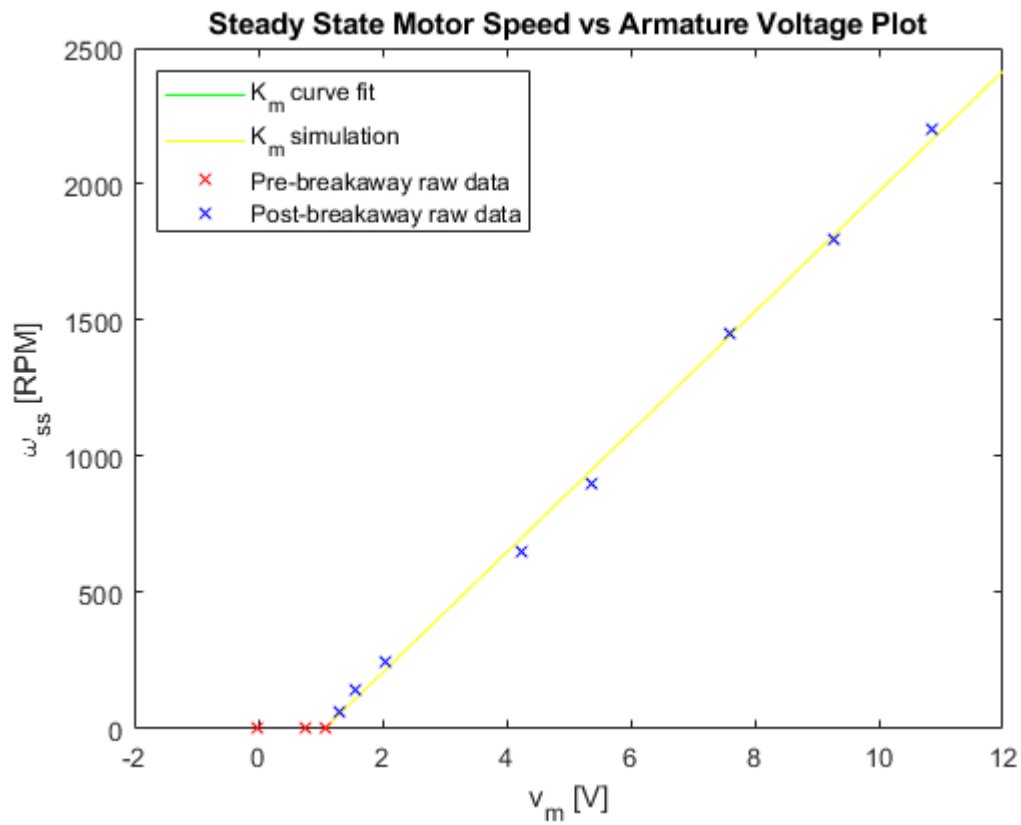
To illustrate that the transient response characteristics are captured by the model, the three experimental step responses are simulated and compared to the raw data.

Step 1 Comparison

Step 2 Comparison

Step 3 Comparison
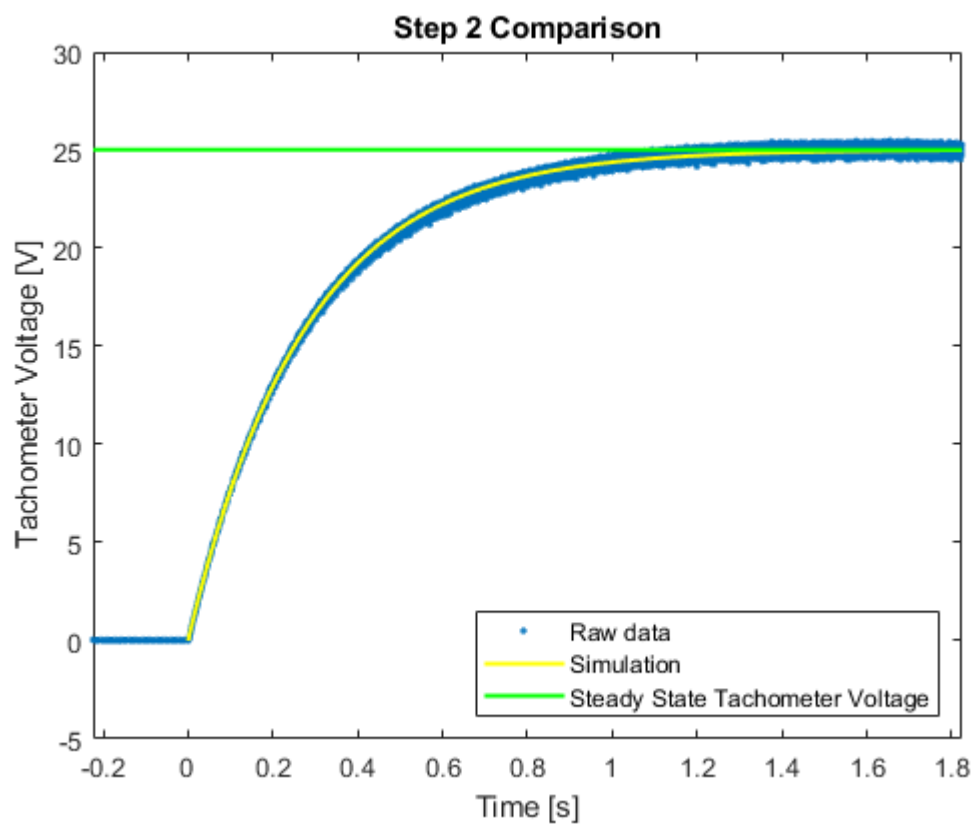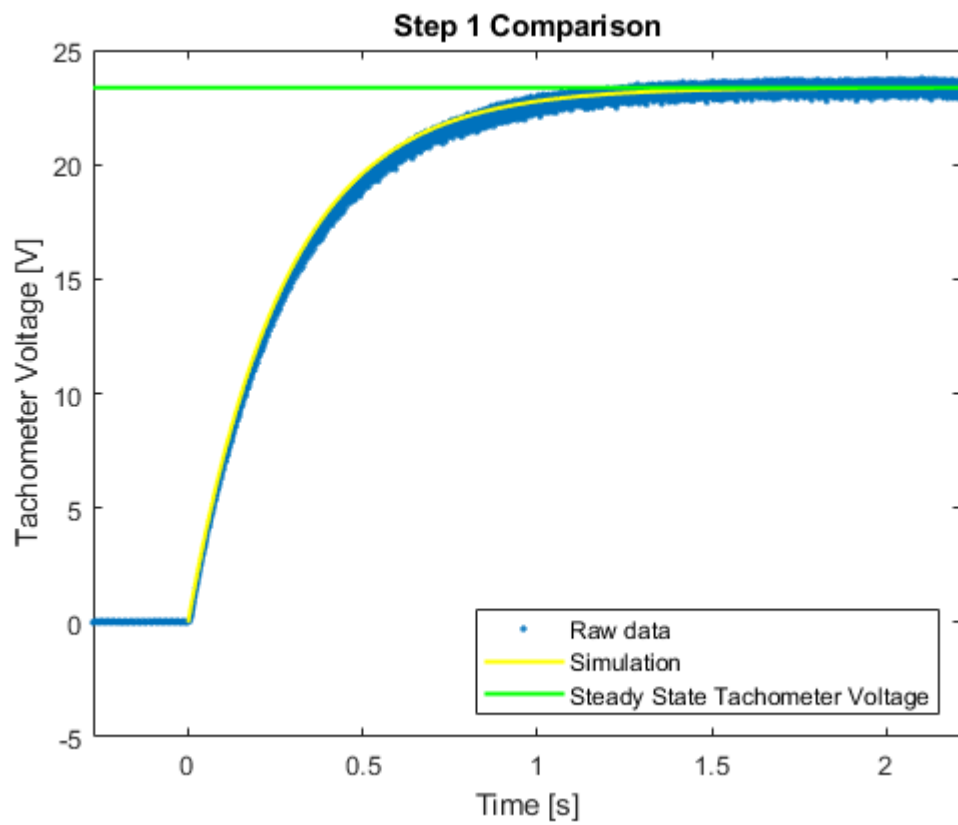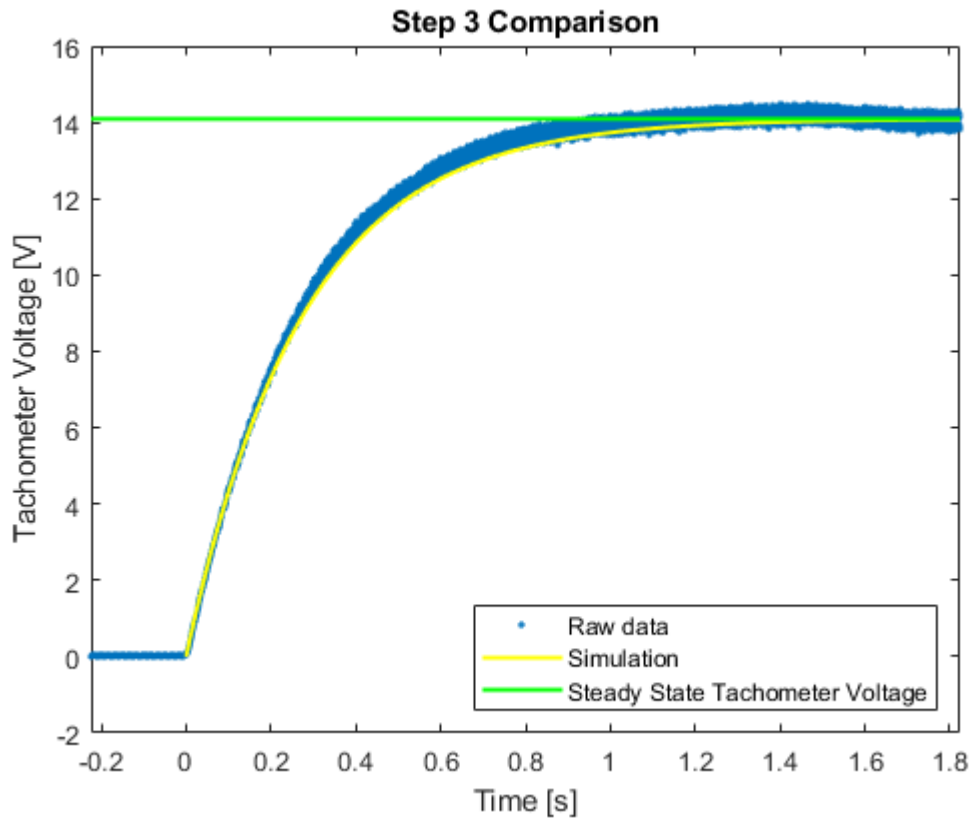
All three step responses match up very well with the experimental data. They all lie within the spread of the data, and they all approach the approximation of the steady state tachometer voltage. It is concluded that the motor modelling is, at least partially, successful. Meaningful conclusions can be drawn from the simulations below, so long as the influence of the pendulum is modelled well enough.

Linear Quadratic Regulator Design

The Q and R matrices are initially chosen to give the $\dot{\theta}$ state about a quarter of the weighting of the θ state. The controller shouldn't care so much if the pendulum moves quickly - what's more important is that the controller regulates it to the upward position. The R matrix is given a heavy weighting so as not to saturate the actuator. A controller that tries as hard as it can initially and then as hard as it can when the position overshoots might not actually be bad - but the design criteria will be for this not to occur. The initial input should land close to the 15V rails of the inverting power amplifier to allow for timeliness/aggressiveness of the response, but it will be capped at 10V for our purposes.

LQR Simulation 1 - Linear System Model

Initially, weighting matrices are chosen as follows

$$Q = \begin{bmatrix} 1 & 0 \\ 0 & 0.2500 \end{bmatrix}$$

$$R = 5$$

Resulting in a gain matrix

$$K = \begin{bmatrix} 1.4572 & 0.3612 \end{bmatrix}$$

Results of the LQR regulation control scheme produce a slow response and a much softer actuation than allowed by the proposed design criteria.

Response Initial LQR Weights - Linear Model
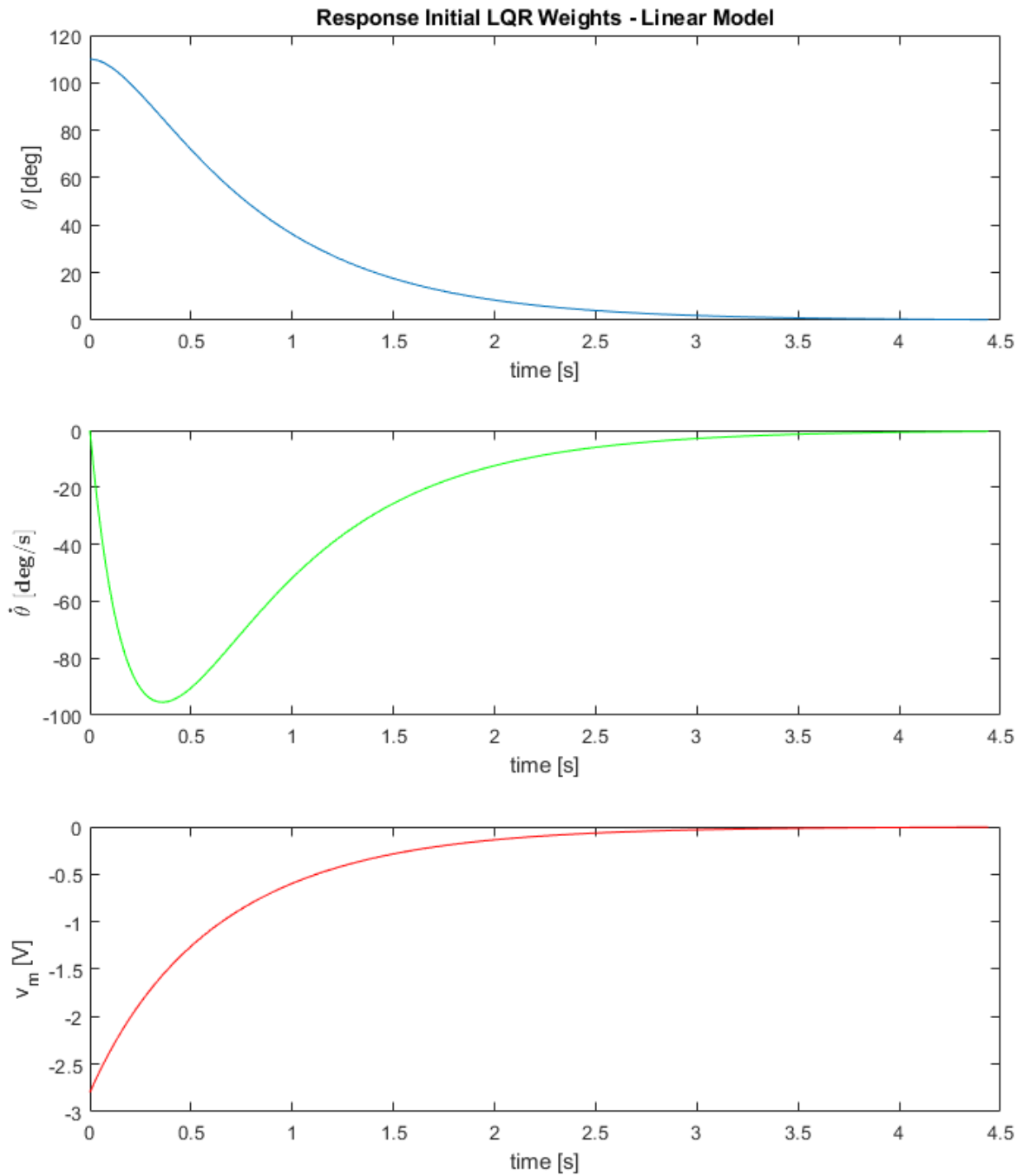
The response settles out at about 4 seconds and the maximum actuation is only, roughly -2.75 V. This control law did not come close enough to the desired 10V.

LQR Simulation 2 - Linear System Model

The position error weighting is made even larger in anticipation of stiction effects in the nonlinear system. The actuation weighting is greatly decreased until the initial actuation is about 10V.

$$Q = \begin{bmatrix} 10 & 0 \\ 0 & 0.2500 \end{bmatrix}$$

$$R = 0.45$$

Resulting in a gain matrix

$$K = \begin{bmatrix} 1.4572 & 0.3612 \end{bmatrix}$$

Response 2 Iterated LQR Weights - Linear Model
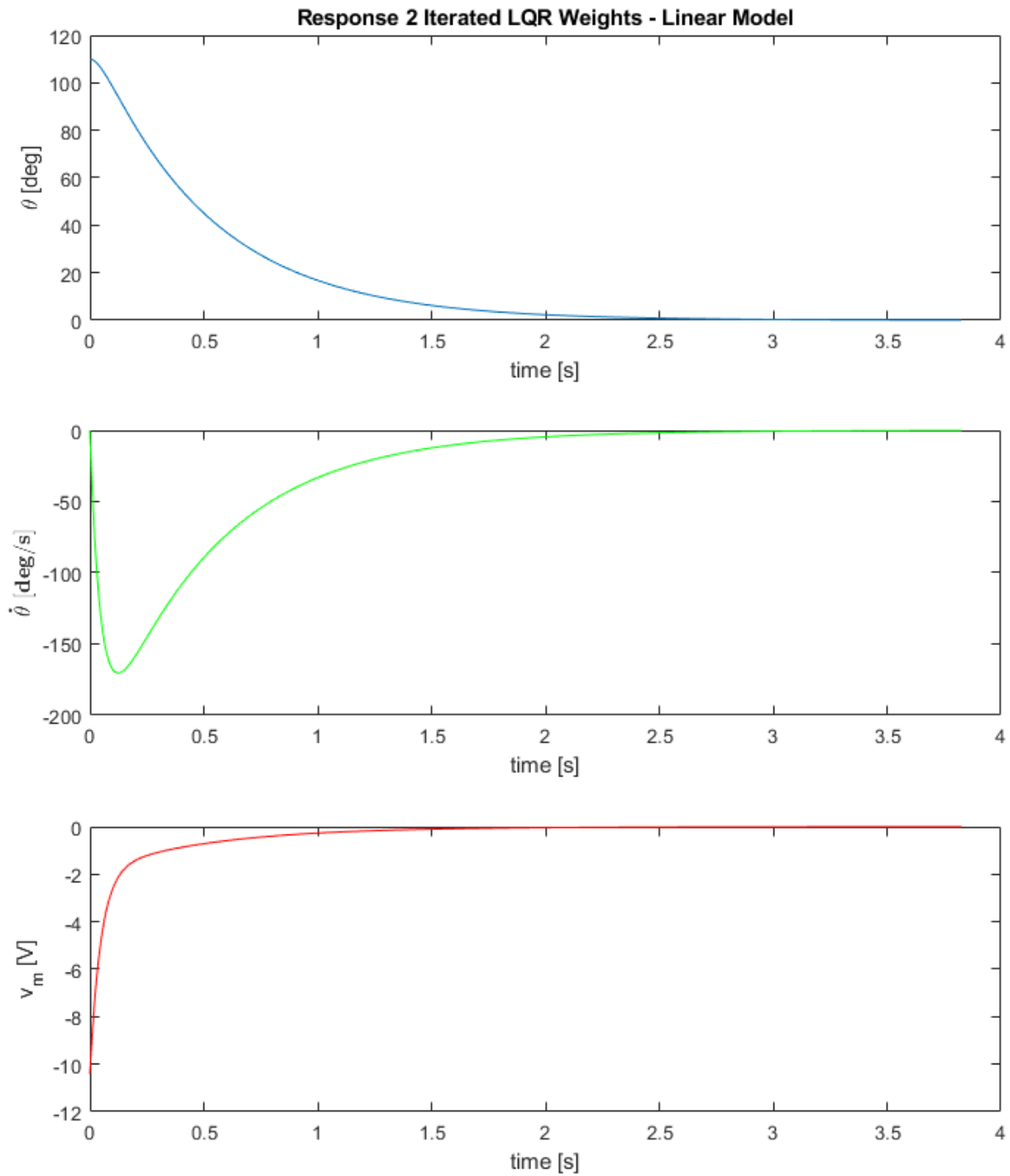
This response achieves the 10V design goal and is tested on the nonlinear system below.

Simulation of the LQR Controller in the Nonlinear System

The Nonlinear Simulink implementation considers the measurement gains, the inverting op amp, and the inverting power amplifier.
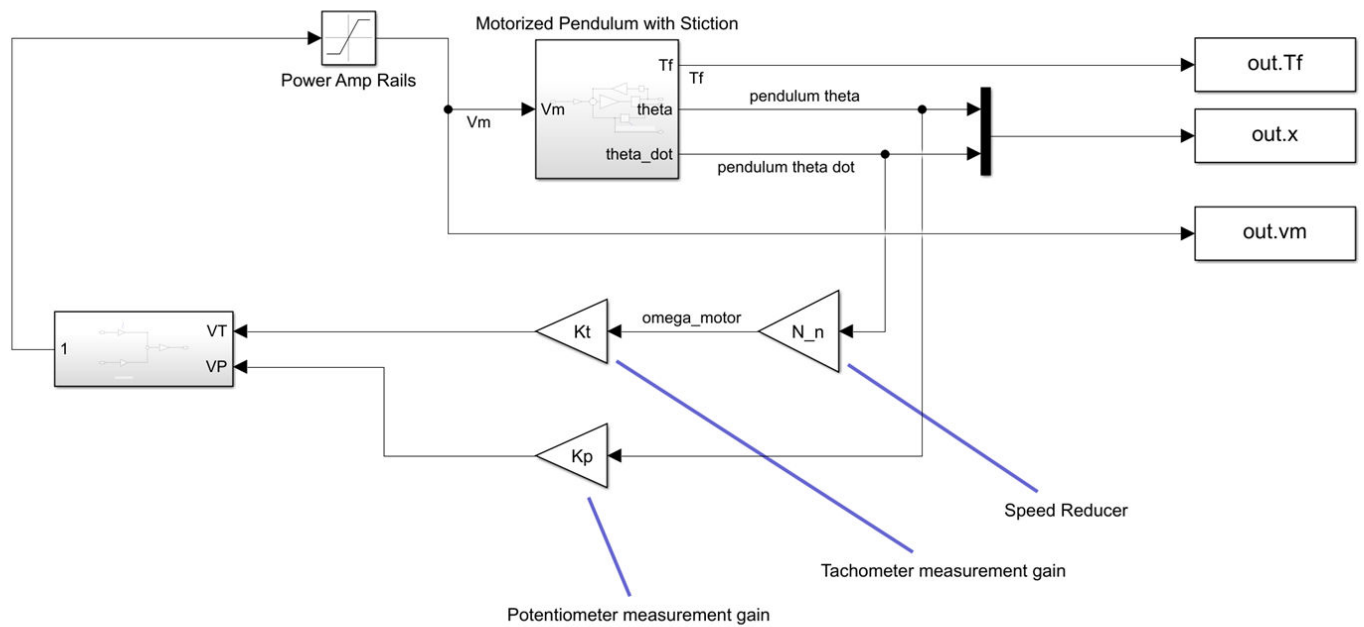
Where the "Motorized Pendulum with Stiction" subsystem contains the equations of motion in pendulum θ states
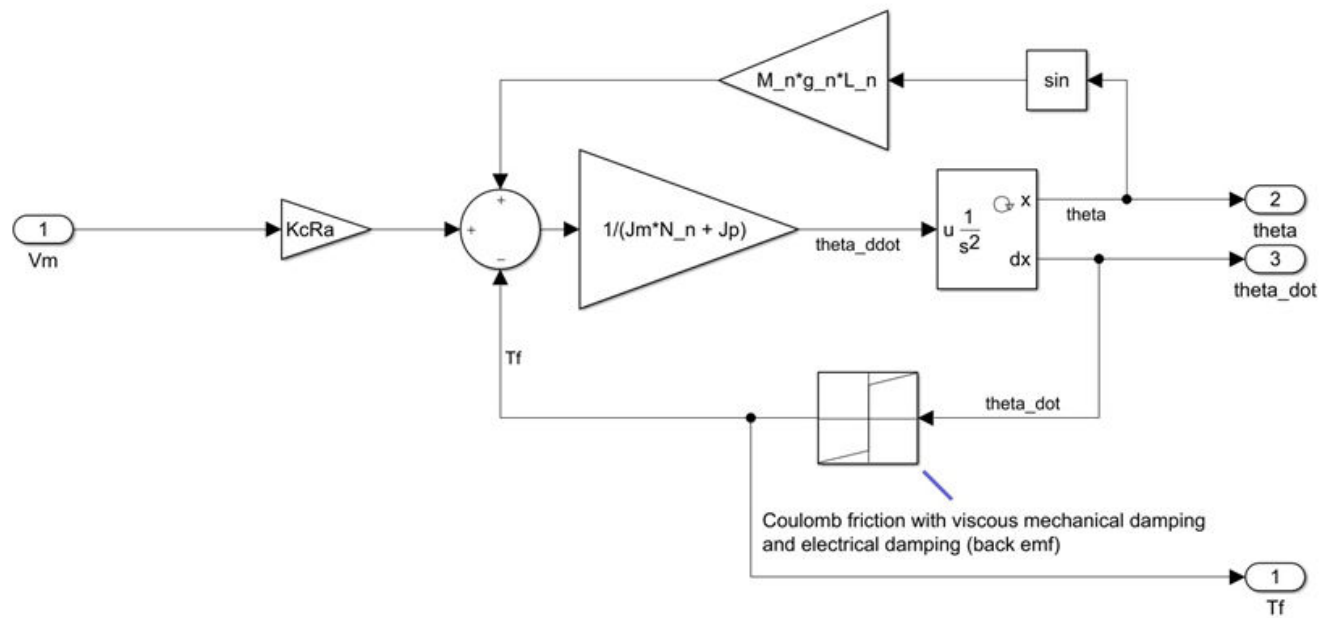
and the "Inverting Op Amp and Inverting Power Amplifier" subsystem contains the op amp gains associated with the physical hardware. The LQR gains must take these into account as well as the measurement gains.
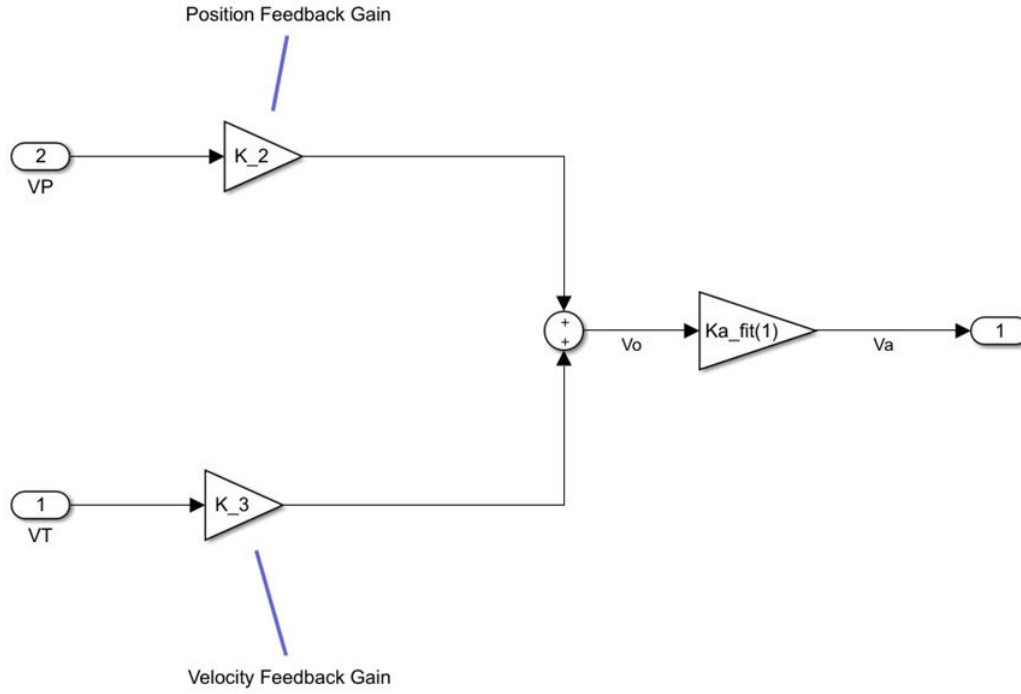
The LQR gains are altered in their sign to account for the inverting nature of the op amp, they are divided by their respective measurement gain (including the gear ratio), and they are again divided by the inverting power amplifier gain. This takes measurements from the true system and converts them into units consistent with the mathematical model.

$$K_2 = -\frac{1}{K_p K_a}[1\ \ 0]K$$

$$K_3 = -\frac{1}{NK_t K_a}[0\ \ 1]K$$

LQR Simulation Nonlinear System - First Attempt

The nonlinear system with stiction is simulated using the Q and R matrices of the second LQR simulation for the linear system. Results are as follows
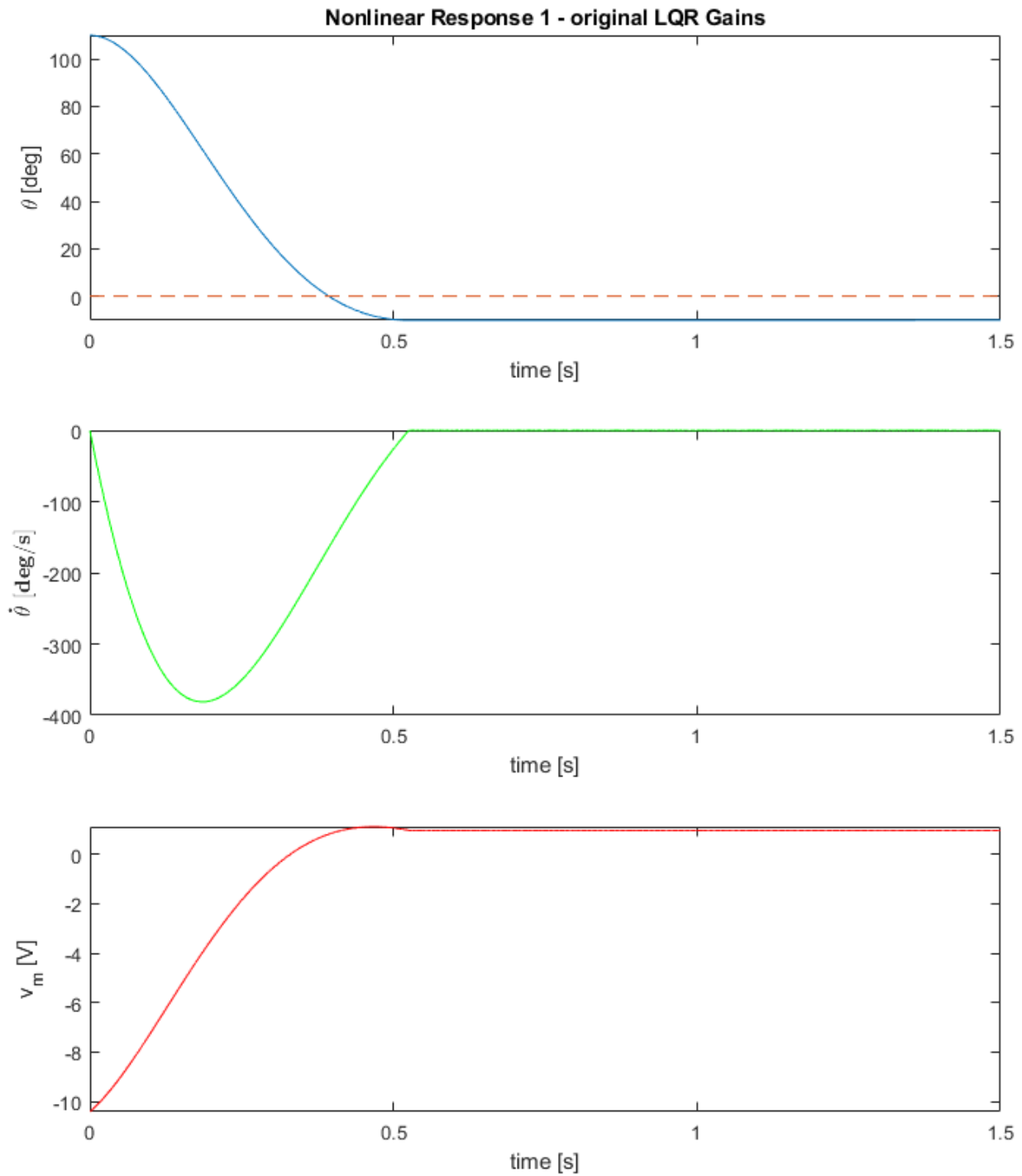
The nonlinear response overshoots the equilibrium point and then gets stuck in stiction at about $-9°$. Further iteration will attempt to mitigate this steady state error - this will be done in the nonlinear system model.

LQR Simulation Nonlinear System - Iterated LQR Gains

LQR gains are chosen as follows

$$Q = \begin{bmatrix} 30 & 0 \\ 0 & 0.2500 \end{bmatrix}$$

$$R = 2$$

Nonlinear Response 2, Iterated LQR Gains
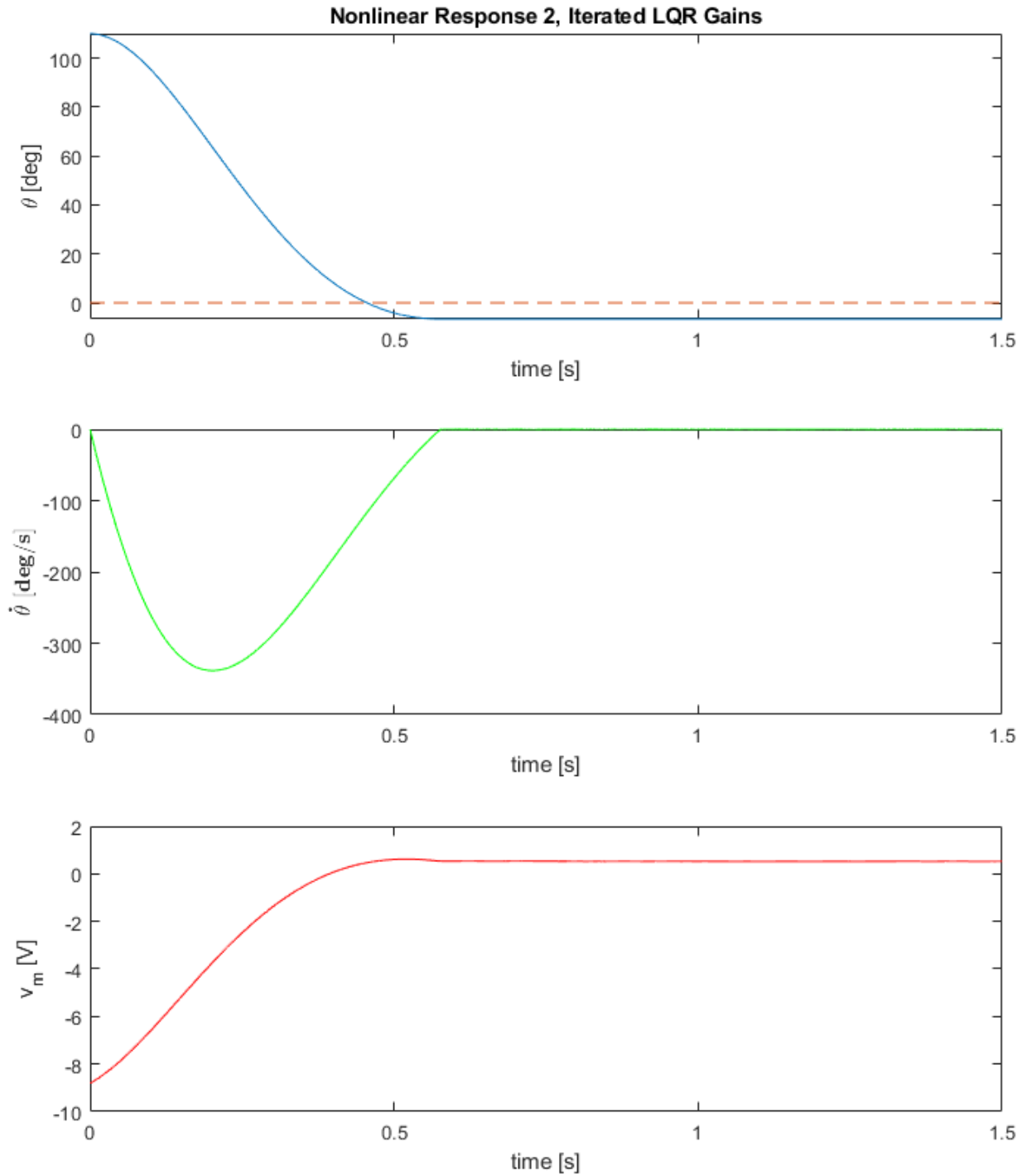
It was found that increasing the position weighting did not fix the steady state error. Rather good results were achieved by decreasing the aggressiveness of the controller until the momentum of the pendulum is close to zero when near the vertical operating point. Essentially, the controller that just so happens to land the pendulum in a stiction region that is close to the operating point is the one that has the best performance. The stiction

keeps the pendulum there, and the position error is too small to overcome it - but the pendulum is close to $\theta = 0$.

LQR Simulation Nonlinear System - Final LQR Gains

A suitable response is found at Q and R matrices

$$Q = \begin{bmatrix} 2 & 0 \\ 0 & 0.2500 \end{bmatrix}$$

$$R = 0.25$$

Nonlinear Response 2, Iterated LQR Gains
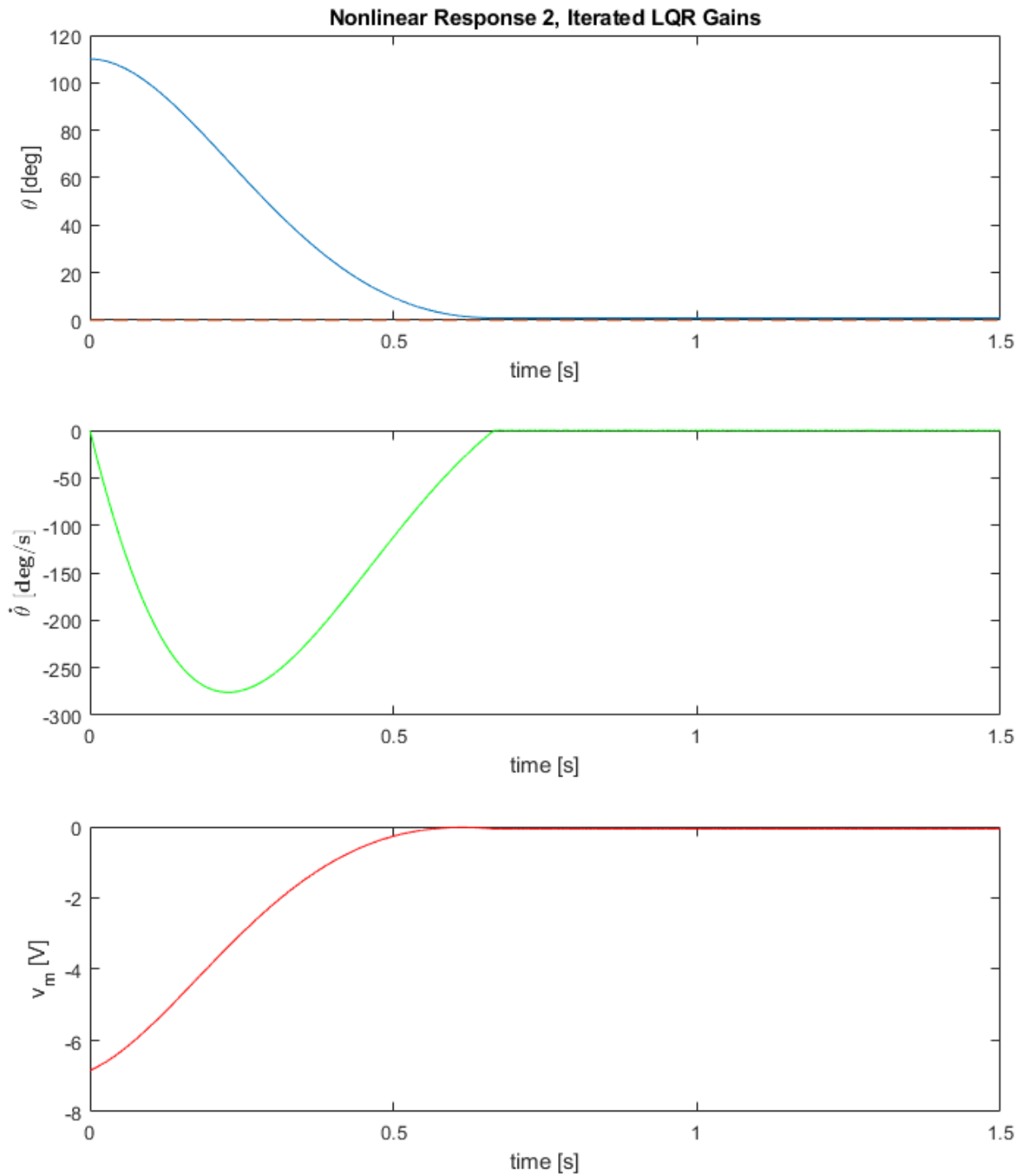
It is found that decreasing R until the pendulum's velocity nears zero when theta is near zero produced a good result. The steady state position error was found to be roughly $0.9°$ which is somewhat close to the upward operating point.

Nonlinear Response 2, Iterated LQR Gains

The static friction takes over here

Linear Controller Discussion

Suitable LQR matrices were found that produce only a small steady state error of around $1°$, given the system's initial conditions. Because the system is nonlinear, the fine tuning of this particular situation will not necessarily hold for a different set of initial conditions. The controller is essentially relying on happenstance for its performance. For the situation where the pendulum is at rest, leaning on the table at $110°$, the controller should work so long as there are no egregious modelling errors.
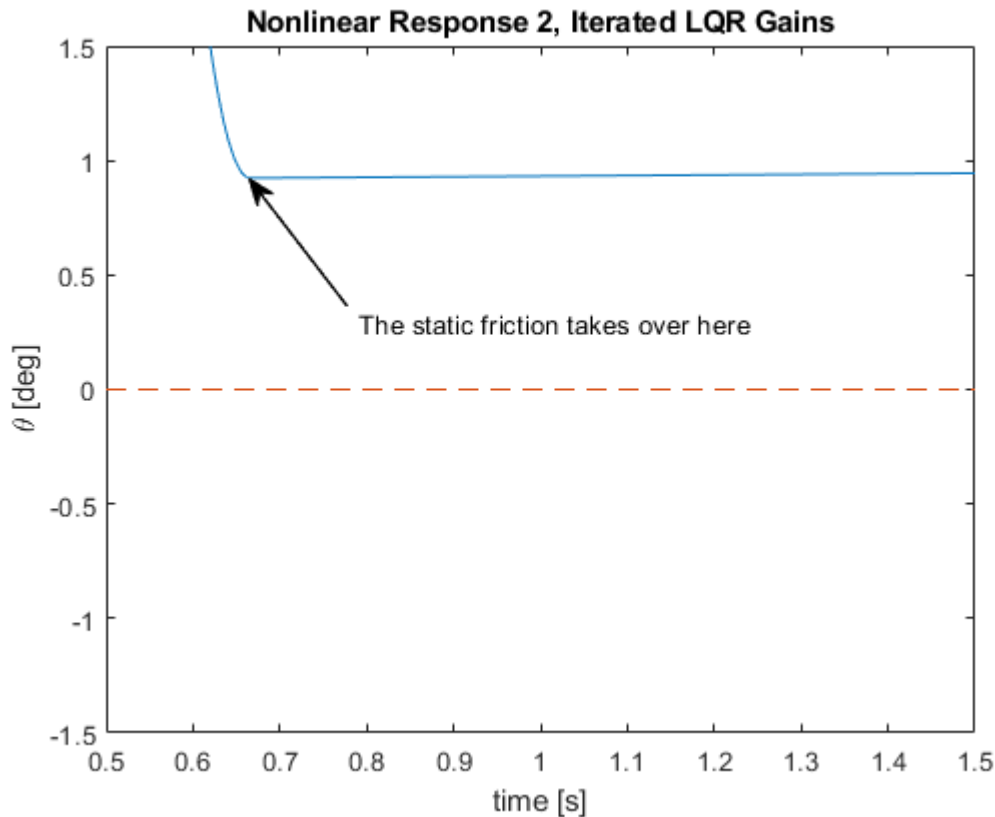
There is only one steady state location that the controller's inability to overcome the stiction is inconsequential - it's the operating point. Any non-zero error will have a stiction force associated with it and if the error is too small, the resultant actuation isn't enough to overcome it. A good first step at making the linear controller work better in the presence of stiction would be to add in some integral action. It would have to be a slow integrator so that it doesn't jolt the system through the stiction and become unstable in that manner, bouncing around equilibrium points in the "sticky" system.

To better determine whether model inaccuracies at large θ values are a problem for a particular K matrix, Lyapunov analysis must be done using methods that consider the size of the region of stability. Since this was not done, any talk of what could potentially cause a stable LQR control scheme to be unstable in its nonlinear implementation is speculative. The major takeaway is that the behavior modelled by the linear representation is drastically different than that of the nonlinear system. This makes iterating on LQR matrices difficult and

unpredictable. A nonlinear control technique, or even linear technique that modifies the LQR method above, is well motivated.

Part Two - Improved Lyapunov Stability Arguments, and Nonlinear Variable Structure Controller

A nonlinear control scheme is desired that can overcome the issue with the LQR approach taken above. The system will take the state from $\vec{x_0} = (110°, 0)$ to the upward operating point within five seconds. It is desired to have a steady state angular error of less than a tenth of a degree, a significant improvements on the original approach. The proposed law has a switching nature, therefore it is desired to prevent chatter in the actuator at steady state - only controllers with no perpetual chattering can be considered successful. Finally, the controller must be robust to model and parameter inaccuracies even in the presence of limited actuation.

$$t_{ss} \leq 5 \; [sec]$$

$$|\theta_{ss}| \leq 0.1 \; [deg]$$

With the model utilized in this paper, the proposed controller satisfies the performance criteria and greatly improves on the steady state error and robustness of the linear quadratic regulator from part 1. The variable structure controller presented is able to take the state from $\vec{x_0}$ to the origin within the required time, within the margin of steady state error, and without actuation chatter. Lyapunov stability arguments that take into account the friction nonlinearity prove that the control law is robust to model innacuracies. This is more compelling than the Lyapunov stability arguments that utilized Lyapunov's indirect method and ignored the stiction. The arguments also provide reasonable certainty that, given the choice of control parameters, the system's stability will not be affected by the actuation rails.

Expanded Lyapunov Stability

The stability analysis in part one utilized Lyapunov's indirect method which had severe limitations. It is desired to utilize a Lyapunov-stability-based control technique that holds for a much larger region of the state space. A control law that is guaranteed to make the desired equilibrium point attractive globally is the ideal scenario. It is shown that this ideal scenario is not achievable with the proposed control law given that the system is effort limited (15 V rails). Additionally, the 100Hz measurement sample rate for the system is not considered in the stability analysis. Rather, it will be compensated for with an additional control structure; a boundary layer that takes over near the switching surface.

Defining Lyapunov Function $V(s)$ and Switching Surface $s(\vec{x}) = 0$

A Lyapunov function $V(s)$ is defined in terms of scalar $s(\vec{x})$ such that it is positive definite. The scalar is defined:

$$s(\vec{x}) = \dot{\theta} + \lambda\theta$$

The equation $s(\vec{x}) = 0$ describes a surface in the state space. On this surface, a decaying linear polynomial in phase variables is realized. If scalar $V(s)$ is defined as:

$$V(s) = \frac{s^2}{2}$$

then $V(s)$ is positive definite. When $V(s)$ is minimized, the system is on the switching surface and the states will decay to zero asymptotically. On the switching surface

$$\dot{\theta} + \lambda\theta = 0$$

and

$$\theta(t + t_{tp}) = e^{-\lambda(t - t_{tp})}\theta(t_{tp})$$

where t_{tp} is the transport time; the time when the system reached the switching surface, and t is the current time.

Negative Definiteness of $\dot{V}(s)$

To prove asymptotic stability, $\dot{V}(s)$ must be negative definite. This is where the control law enters consideration.

A control actuation will be selected such that, through state feedback, $\dot{V}(s)$ can be made negative definite. It is shown here that there are practical limitations to this; but an effective control law can still be designed for the real input limited system.

$$\dot{V}(s) = s\dot{s}(s)$$

where $\dot{s}(s)$ denotes the derivative of $s(\overrightarrow{x})$ formulated explicitly in terms of s. The derivative cannot be formulated in this manner immediately, so for now

$$\dot{s}(\overrightarrow{x}, v_m) = \ddot{\theta}(\overrightarrow{x}, v_m) + \lambda\dot{\theta}$$

The $\ddot{\theta}$ can be written as:

$$\ddot{\theta}(\overrightarrow{x}, v_m) = f(\overrightarrow{x}) + bv_m$$

where

$$f(\overrightarrow{x}) = \frac{L M g \sin(\theta) - T_{ba}\operatorname{sign}(\dot{\theta}) - \dfrac{K_c N \dot{\theta}}{K_m R_a}}{J_m N + J_p}$$

and

$$b = \frac{K_c}{R_a(J_m N + J_p)}$$

And, $\dot{s}(\overrightarrow{x}, v_m)$ becomes:

$$\dot{s}(\overrightarrow{x}, v_m) = f(\overrightarrow{x}) + bv_m + \lambda\dot{\theta}$$

It is desired to eliminate explicit dependance on the state of the nonlinear system from the Lyapunov function's derivative. If $\dot{V}(s)$, which is more generally a function of the state (i.e. $\dot{V}(\overrightarrow{x})$), can be kept in terms of s alone, then the negative definiteness can be a reasoned in a straightforward manner. To achieve this, the nonlinearities of the plant are cancelled out, and $\dot{s}$ is driven to zero, via a nullifying actuation voltage $\widehat{v}$.

$$\hat{\dot{s}} = \hat{f}(\vec{x}) + b\hat{v} + \lambda\dot{\theta} = 0$$

$$\hat{v} = -\frac{1}{b}(\hat{f}(\vec{x}) + \lambda\dot{\theta})$$

where $\hat{f}(\vec{x})$ is the best estimate available of $f(\vec{x})$. Plugging in the system dynamics

$$\hat{v} = \frac{R_a(J_m N + J_p)}{K_c}\left(\frac{-L M g \sin(\theta) + T_{ba}\operatorname{sign}(\dot{\theta}) + \dfrac{K_c N \dot{\theta}}{K_m R_a}}{J_m N + J_p} - \lambda\dot{\theta}\right)$$

or, numerically

$$\hat{v} = 0.3501\,\dot{\theta} + 1.0684\operatorname{sign}(\dot{\theta}) - 0.6600\sin(\theta) - 0.1144\,\lambda\dot{\theta}$$

An additional actuation v_s, formulated as a feedback law on s, is added to $\hat{v}$ to give the total control actuation v_m.

$$v_m = \hat{v} + v_s(s)$$

Using this input, $\dot{s}$ is

$$\dot{s}(\vec{x}, \hat{v}, s) = f(\vec{x}) + b(\hat{v} + v_s(s)) + \lambda\dot{\theta}$$

$$\dot{s}(\vec{x}, s) \;=\; f(\vec{x}) - \widehat{f}(\vec{x}) - \lambda\dot{\theta} + bv_s(s) + \lambda\dot{\theta}$$

$$\dot{s}(\vec{x}, s) \;=\; F(\vec{x}) + bv_s(s)$$

First Practical Limitation on Proof of Negative Definiteness - Model Uncertainty

Above, F represents a mismatch between the model and the real system. This is not a completely satisfactory result because $\dot{s}$ is not a function of s alone. Therefore, the model uncertainty is the first limitation on a proof of negative definiteness that encorporates a feedback law on s.

$$\dot{V}(\vec{x}, s) \;=\; s(F(\vec{x}) + bv_s) \;<\; 0$$

i.e.

$$sbv_s \;<\; -sF(\vec{x})$$

If v_s is not made large enough in magnitude, this inequality will surely fail.

Second Practical Limitation on Proof of Negative Definiteness - Saturated Actuation

The second limitation comes from the voltage rails. The bounds on the actuation are $\pm 15V$,

$$|v_m| \;=\; |\widehat{v} + v_s| \leq 15[V]$$

A trajectory requiring too much nullifying voltage at any point in time will saturate the actuator and v_s will have additional requirements to satisfy negative definiteness. When this happens, $\widehat{\dot{s}} \neq 0$ and

$$\widehat{v} \;=\; -\frac{1}{b}\left(\widehat{f}(\vec{x}) + \lambda\dot{\theta}\right) + \frac{1}{b}\widehat{\dot{s}}$$

$$\dot{s}(\vec{x}, s) = F(\vec{x}) + \hat{\dot{s}} + bv_s(s)$$

$$\dot{V}(\vec{x}, s) = s(F(\vec{x}) + \hat{\dot{s}} + bv_s(s)) < 0$$

Where now the condition for negative definiteness is affected by the value of $\hat{\dot{s}}$. This report will not address the possibility of reducing the model uncertainty, but λ and a switching gain K will be tuned manually to ensure that, for our scenario, $\hat{\dot{s}}$ is zero and $\hat{v}$ stays far enough away from $\pm 15V$.

## Nonlinear Variable Structure Controller Design

A control law with two meta-structures is proposed. The first is a switching law for v_s that keeps $s = 0$ attractive in the presence of model uncertainty.

$$v_s = -\frac{K}{b} sign(s)$$

The second is a smoothing proportional controller on s that is implemented near a boundary layer. The discrete measurements available for feedback are shown to produce chatter in the actuator and an undesirable amount of swinging about the equilibrium point. If the aggressiveness is slowed down near the switching surface, this chatter is reduced or eliminated.

$$v_s = -C_{BL}\frac{K}{b}s$$

The combination of the meta-structures is implemented as a saturation control law with suitably chosen pre and post-multiplying gains. The pre-multiplying gain C_{BL} will control the size of the boundary layer along with the aggressiveness of the linear control law on s. The post multiplying gain $\frac{K}{b}$ will control the magnitude of the switching law outside the boundary layer.

Switching Control Law With Boundary Layer: First Two Meta-Structures
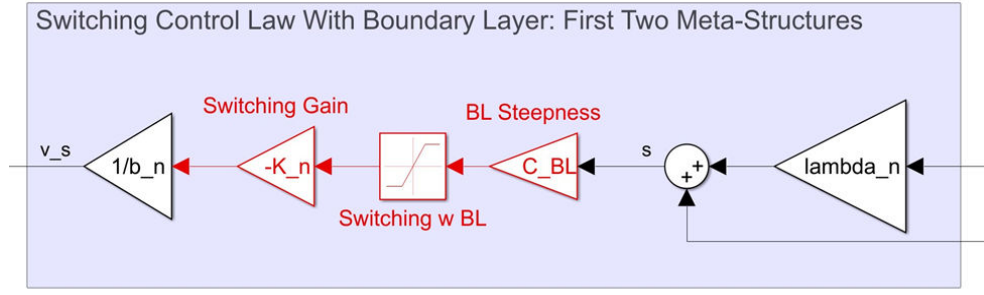
Switching Control Law

If the $\widehat{v}$ condition is satisfied for a particular trajectory, then negative definiteness is, in part, determined by how much actuation is left over from the rails. The more of the remaining voltage v_s utilizes, the more attractive the switching surface becomes. This must be balanced though, because a larger switching voltage may make the nullifying voltage exceed the design specifications. If there is always enough voltage leftover from $\widehat{v}$ to combat the uncertainties, and $\frac{K}{b}$ is large enough, then the proposed signum switching law's $\dot{V}$ is negative definite for the trajectory.

$$v_s = -\frac{K}{b} sign(s)$$

$$\dot{V}(\overrightarrow{x}, s) = s(F(\overrightarrow{x}) - Ksign(s)) < 0$$

$$sKsign(s)) > sF(\overrightarrow{x})$$

$$K|s| > sF(\overrightarrow{x})$$

where

$$|v_m| = |\widehat{v} - \frac{K}{b} sign(s)| \leq 15[V]$$

any amount of v_s that exceeds what the actuator can provide will reduce the control law's ability to combat the model uncertainties. With F = 0 however, there is no limitation on $|v_s|$ (so long as the $|\hat{v}| < 15V$ condition holds).

**Switching Control Law Simulations**

Simulation 1

Using $\lambda = 45$ and $\frac{K}{b} = 10$, a suitable trajectory is found from the initial conditions that keeps $\hat{v}$ within the rails. Initially, the system is simulated with a very large meaurement sample frequency of 100KHz.

## Switching Law, No Boundary Layer, 100KHz Sample Frequency
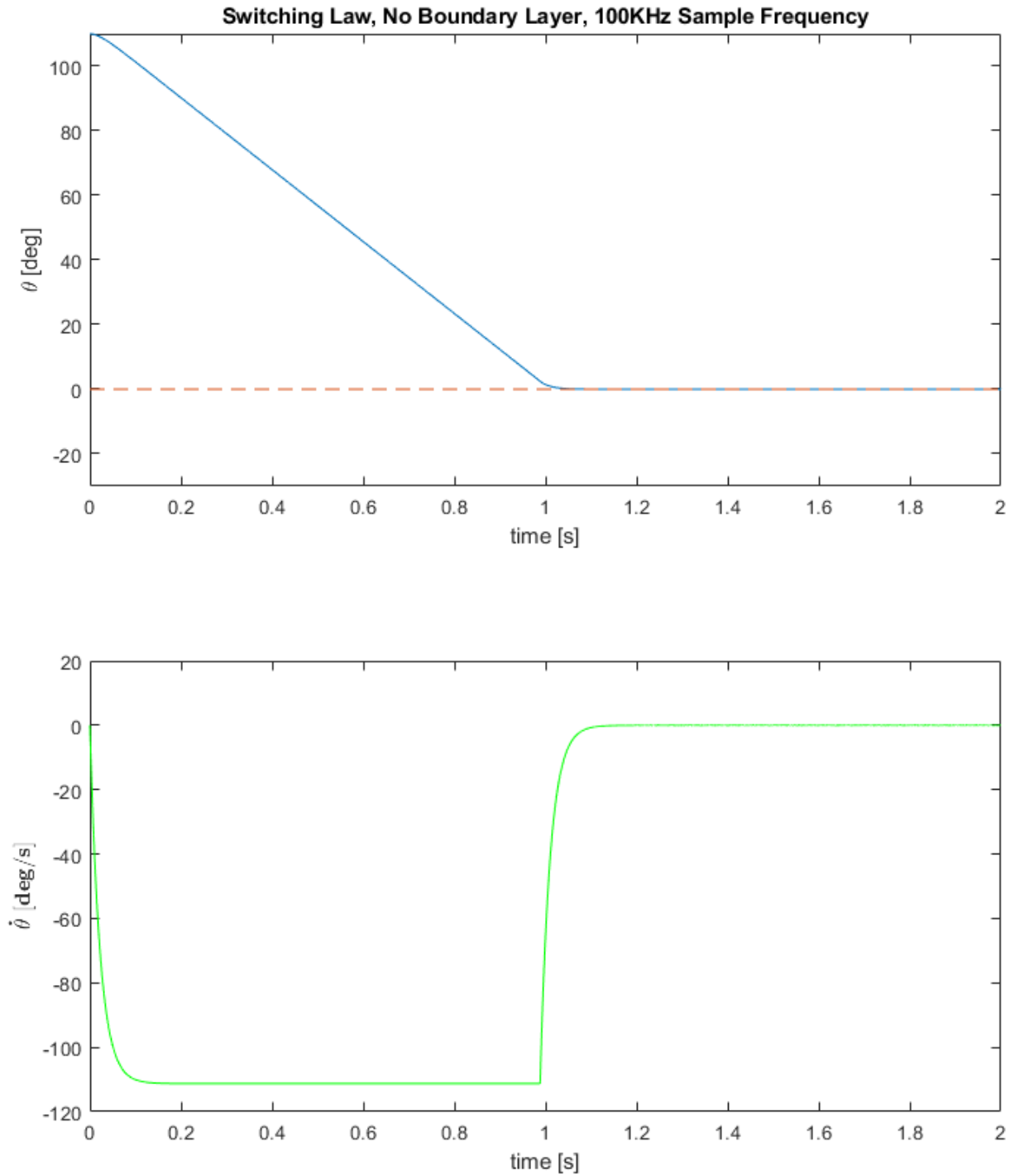
The performance in this simulation is excellent. This is due to the ability of the actuator to react very quickly to deviations from the switching surface. The controller reaches a θ error of about $0.5°$ at around 1.15 seconds satisfying the 5 second design requirement. The θ steady state error requirement is also satisfied.

```
Steady state angular error was about 8.1e-05 [deg]
```

However, there is still a bit of velocity chatter occuring at 100KHz. If the switching were infinitely fast, this would not be present, but this is not realizable in simualtion or in implementation. Regardless, the system sways back and forth with a very small velocity that averages to zero.
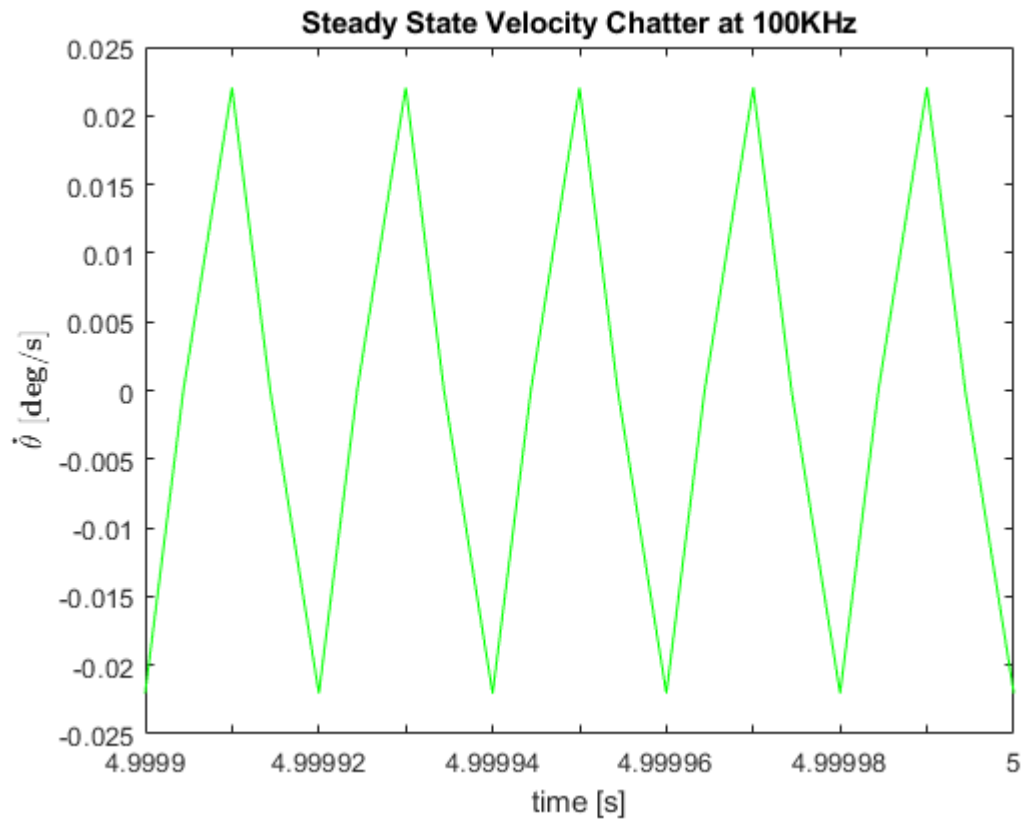

The nullifying voltage is shown to be within $\pm 15V$, so that design criterion is satisfied. However, a consequence of this performance is that the actuation chatters rapidly. This is to be expected with a switching law, but partly motivates the addition of a boundary layer.

**100KHz Response, Nullifying Voltage and Actuation Chatter**
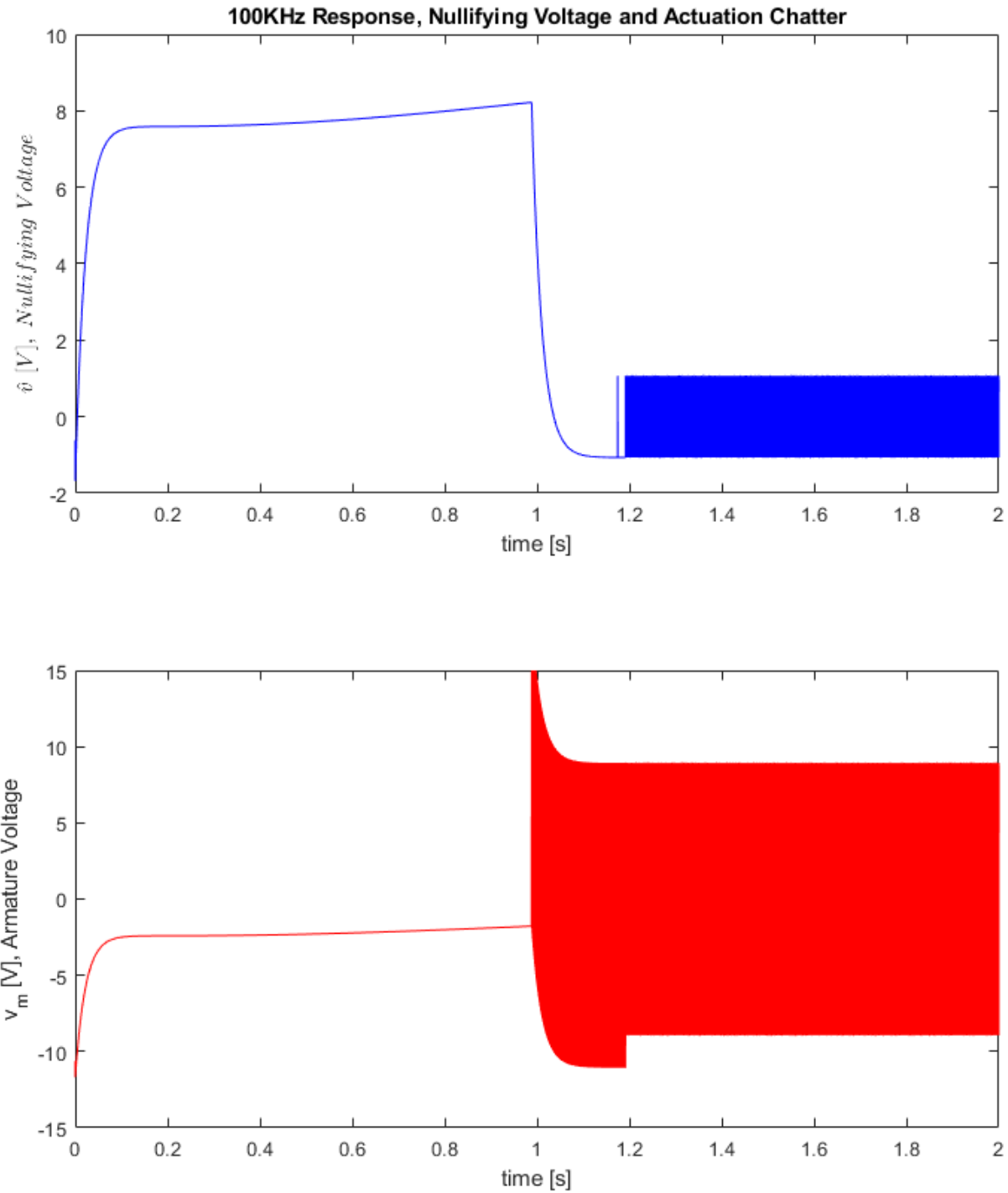
The use of a 100KHz sample rate is not realistic - the hardware implementation has as much slower sample rate of 100Hz. In simulation 2, this will be simulated using the same switching law that produced these initial results.

Simulation 2

$\lambda = 45, \frac{K}{b} = 10$, ran at 10Hz

Switching Law, No BL, 100Hz Sample Time
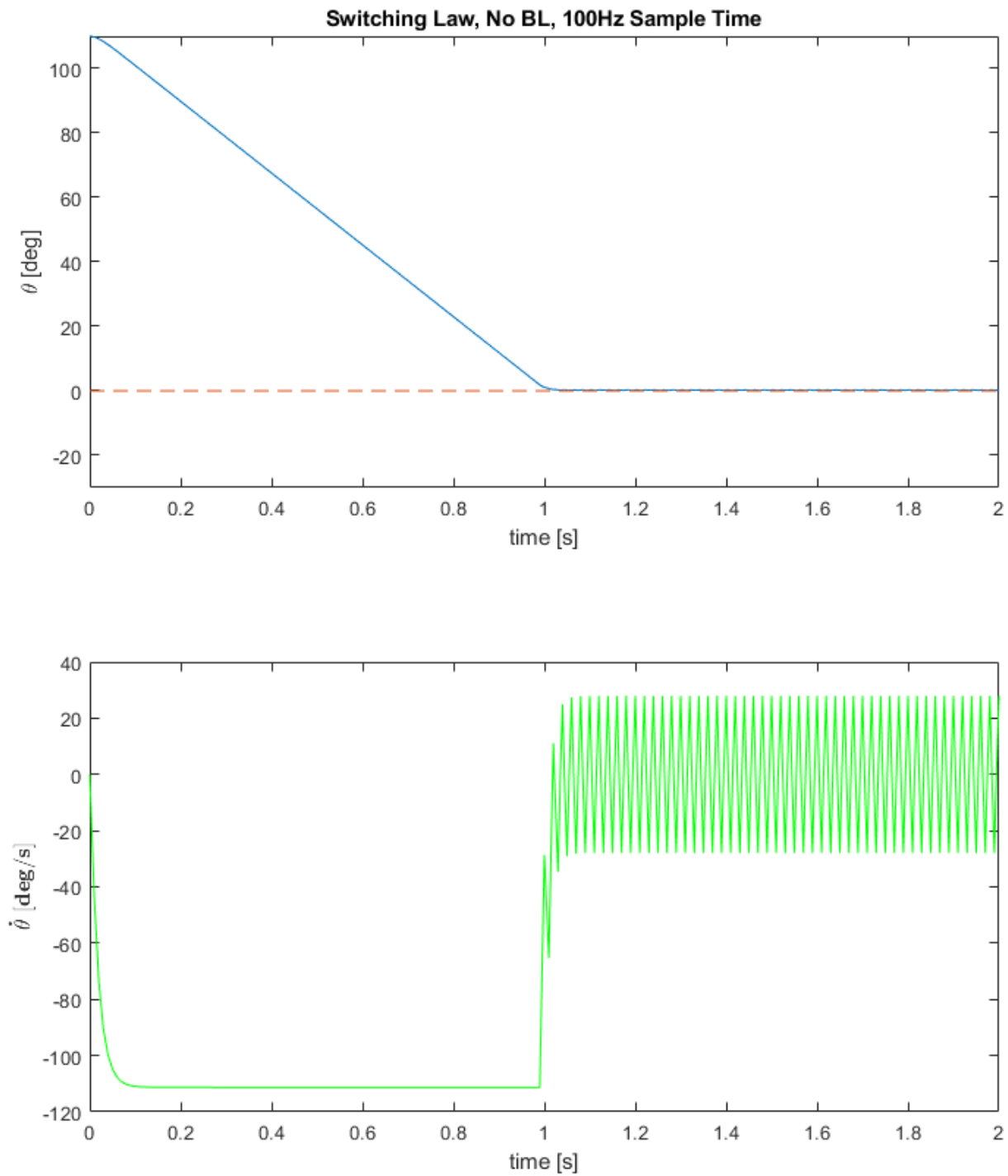
Around the switching surface, the control law's performance is significantly degraded at the reduced sample frequency. The system does not asymptotically stabilize and it sways about the operating point at 100Hz.
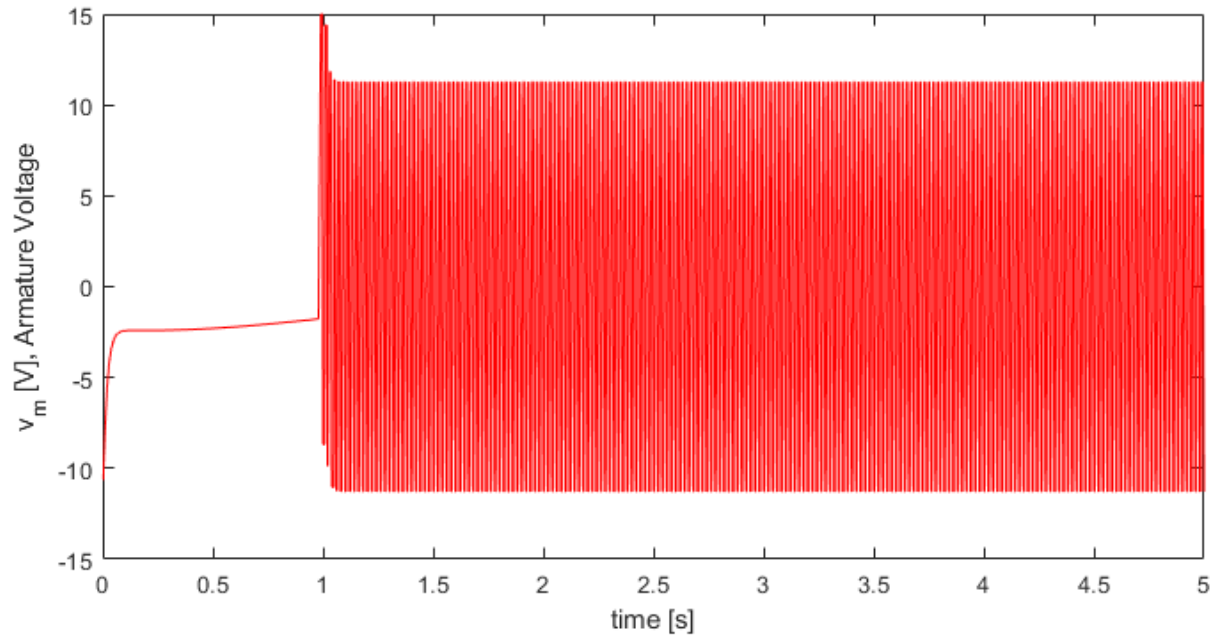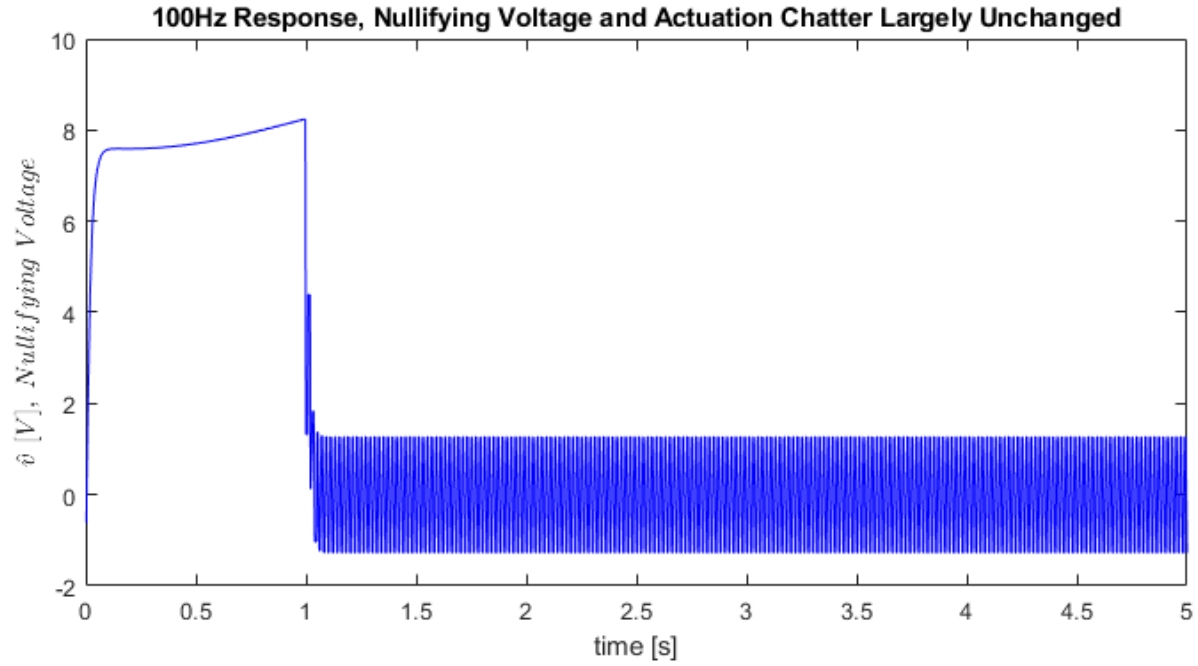
The actuation chatter is still present as well - the nullifying voltage and armature voltage are slightly different but overall, represent the same bulk behavior as the higher frequency case. The λ and $\frac{K}{b}$ values are still suitable for the sample rate present on the hardware. To reduce the actuation chatter, a smoothing boundary layer is introduced.

Smoothing Boundary Layer

Near the operating point, at $\dot{\theta}$ gets smaller and smaller, the nullfying voltage begans to be dominated by the coulomb friction term $T_{ba}sign(\dot{\theta})$. The voltage associated with this is $V_{ba} = 1.07V$ which is far from the rails. This will, however, be influenced by the size of the boundary layer. For a small enough boundary layer, it is of little concern how $\hat{v}$ is behaving and the design criteria can focus on two requirements:

1. Keeping v_s large enough in magnitude to ensure negative definiteness.
2. Smoothing out the response enough in the boundary layer to eliminate the 100Hz discretization-induced chatter.

The first design requirement is going to affect the steady state error in the presence of model uncertainty. The second requirement is about the discrete system's convergence/stability. Neither of these requirements will be approached analytically. Rather, the boundary layer steepness coefficient C_{BL} will be tuned while keeping the system parameters from previous successful simulations.

The smoothing boundary layer control law

$$v_s = -C_{BL}\frac{K}{b}s$$

has the following negative definiteness requirement:

$$\dot{V}(\vec{x},s) = s(F(\vec{x}) - C_{BL}Ks) < 0$$

$$C_{BL}Ks^2 > sF(\vec{x})$$

This can be further simplified since $C_{BL}Ks^2$ is positive definite, any negative or zero value of $sF(\vec{x})$ automatically satisfies the inequality. Therefore only the case where s and $F(\vec{x})$ have the same sign needs to be considered.

$$C_{BL}K|s| \; > \; |sF(\vec{x})|$$

$$C_{BL}K \; > \; |F(\vec{x})|$$

So, if $C_{BL}K$ is larger than the magnitude of the model uncertainty at every point along a boundary layer trajectory, the system will be negative definite. In the continuous case, the boundary layer, $s = 0$ is attractive given this requirement. In the discrete case, however, successive actuations held constant over the sample period must produce a subsequent state that is smaller than its predecessor. A full nonlinear discretization that includes the imperfect nature of the nullifying actuation is impractical, which motivates an iterative tuning method for C_{BL}. It is desired to find as large a value as possible before the system loses its discrete stability. Additionally, a design factor will be added to make the boundary layer a bit larger in an attempt to prevent the system from overshooting the boundary layer completely.

Switching Control Law with Boundary Layer Simulations

Simulation 3

Using $\lambda \; = \; 45$, $\dfrac{K}{b} \; = \; 10$, and $C_{BL} = 2$ a marginally suitable control response is found that eliminates actuation chatter at steady state.

Switching Law With Boundary Layer, 100Hz Sample Time, C_{BL} = 2
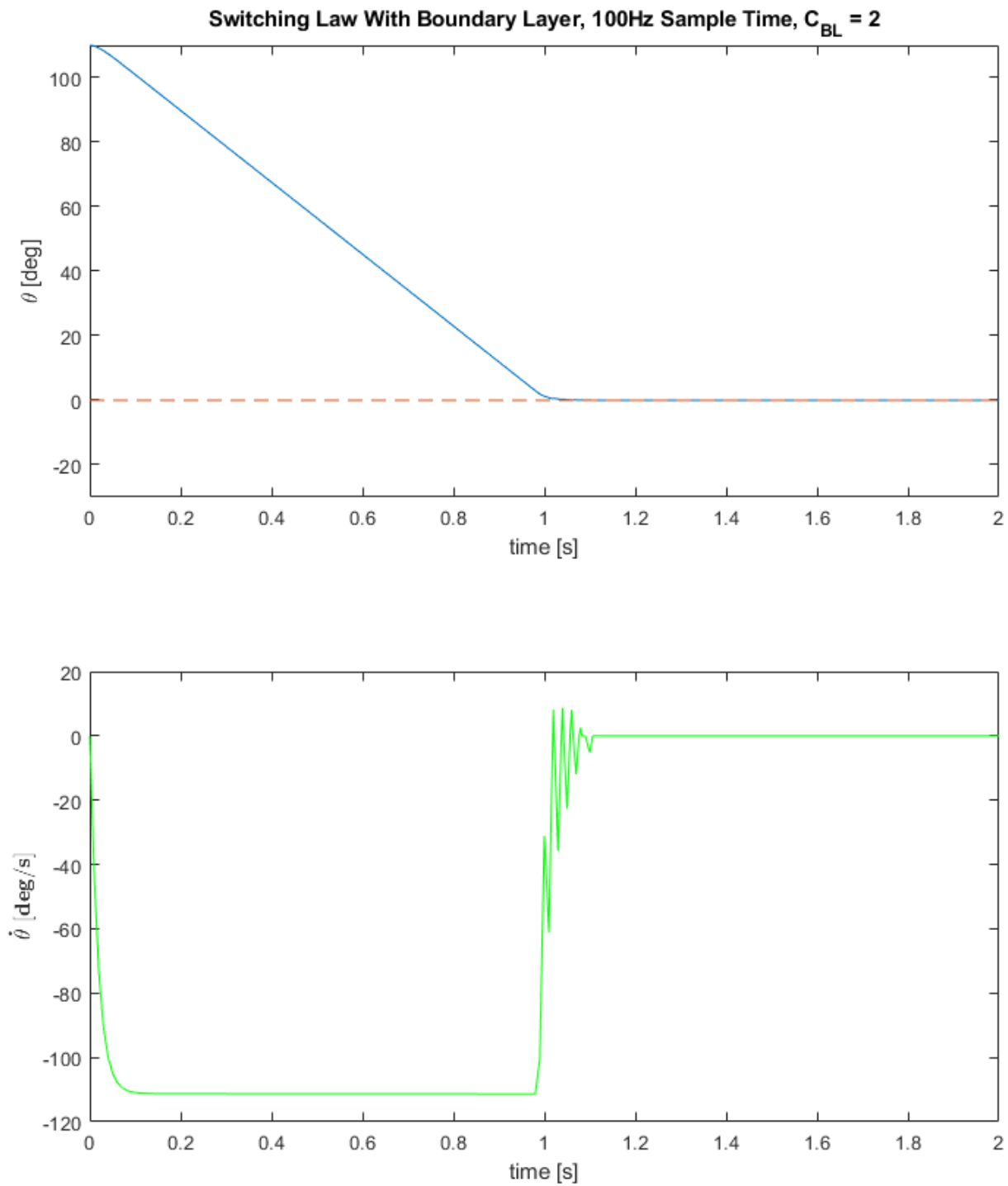
There is quite a bit of oscillation around the boundary layer before the system eventually gets brought in completely. It is evident that the low sample rate is responsible for this as the velocity oscillation occurs at 100Hz.

Oscillation Around Boundary Layer, $C_{BL} = 2$
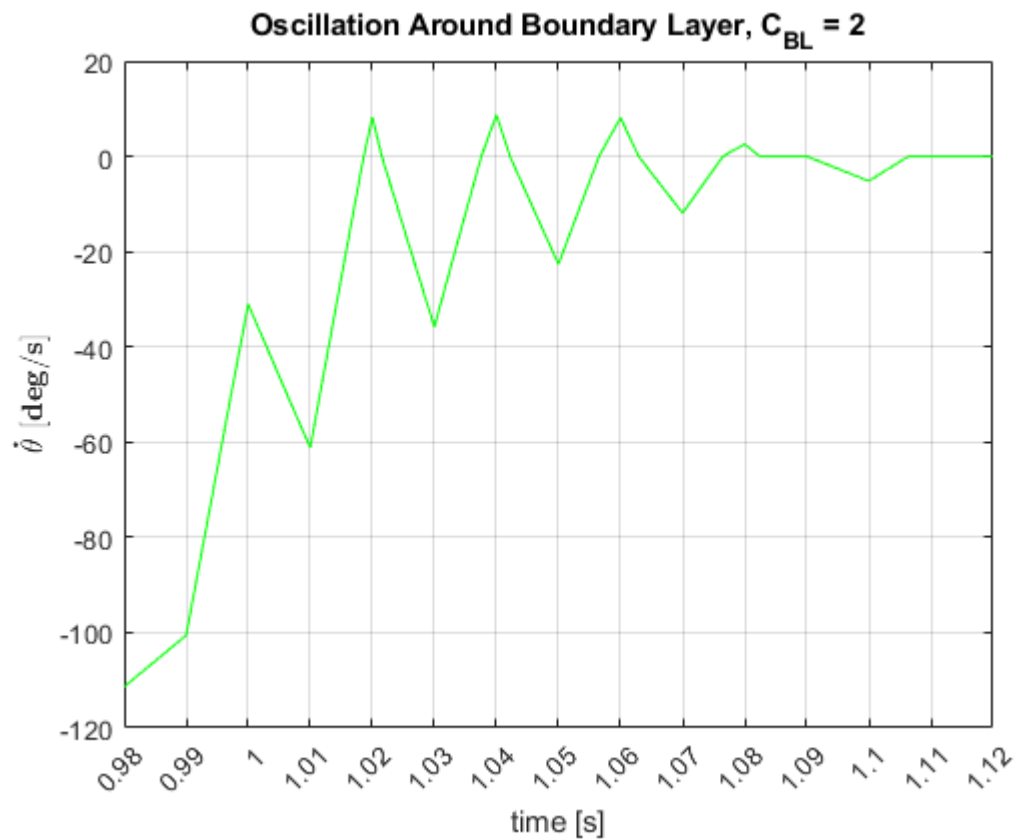
Raising the value to just 2.2 causes the system to overshoot the boundary layer too violently and enter a state of perpetual switching.

Simulation 4

Using $\lambda = 45$, $\dfrac{K}{b} = 10$, and $C_{BL} = 2.2$ an unsuitable control response is found that does not eliminate actuation chatter at steady state. An approximate upper limit on C_{BL} is shown to be about 2.

Switching Law With Boundary Layer Only, 100Hz Sample Time, $C_{BL} = 2.2$
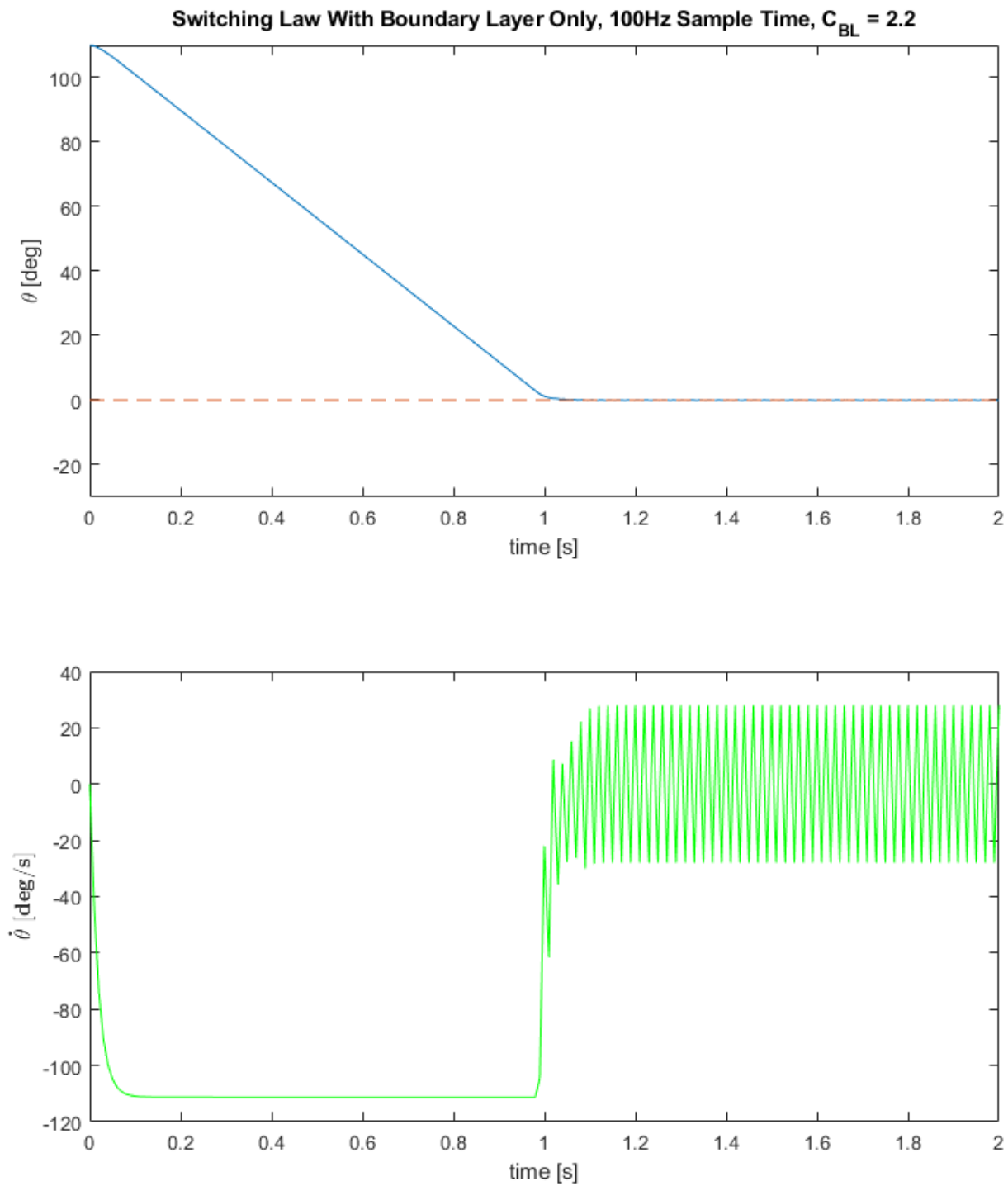
Here, the discretization chatter has taken over and the system oscillates about the equilibrium point at 100Hz. Setting the boundary layer coefficient to 1 produces much better results, and will be utilized in the finalized control law below.

Finalized Control Law

Simulink Implementation
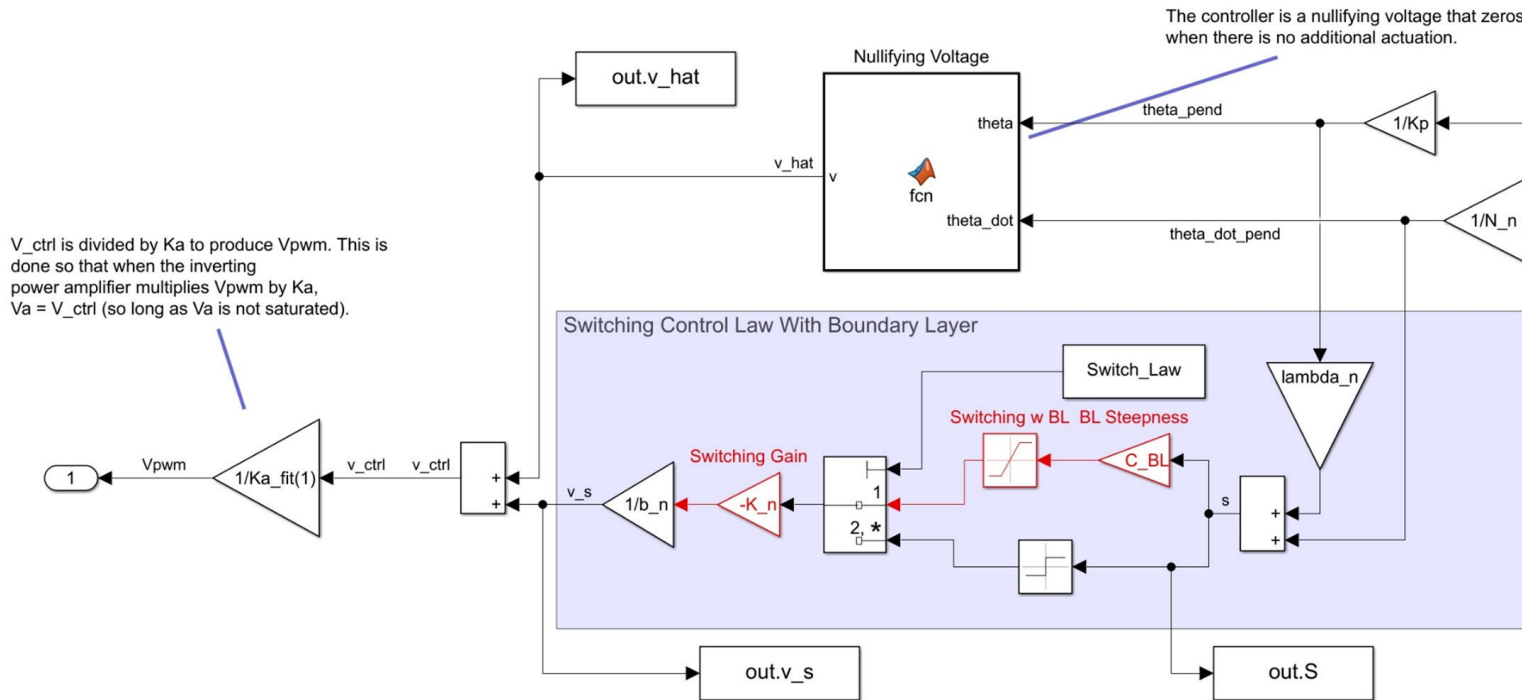
Here, the nullifying voltage contains the numerical expression determined in the above Lyapunov analysis.

```
function v = fcn(theta, theta_dot, lambda_n, K_n)


v = 0.3501*theta_dot + 1.0684*sign(theta_dot) - 0.6600*sin(theta)...
      - 0.1144*lambda_n*theta_dot;
```

The saturation nonlinearity saturates at ± 1 and its switching magnitude is given by K_n. The boundary layer coefficient C_BL premultiplies the nonlinearity so that it only affects the slope (and consequently the size) of the boundary layer. The state vector is measured in volts at a frequency of 100Hz and it brought into the correct units through Kp, N_n, and Kt. The actuation is scaled by Ka so that v_ctrl represents the desired armature voltage v_m. The plant provides the actuation saturation as it did in part 1.

Simulation of Finalized Control Law - Prediction of Hardware Behavior
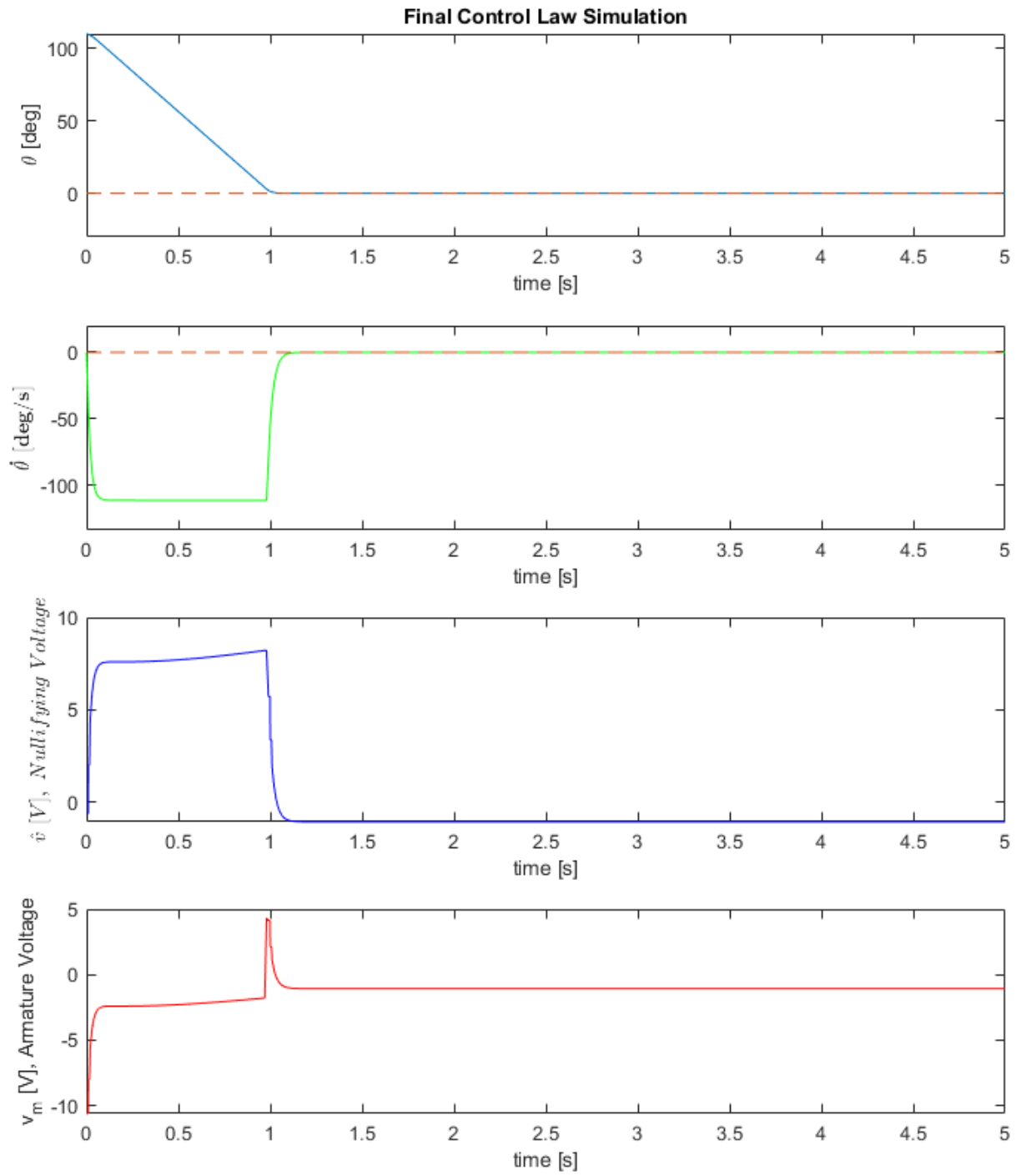
The finalized control parameters are

$$K = 10$$

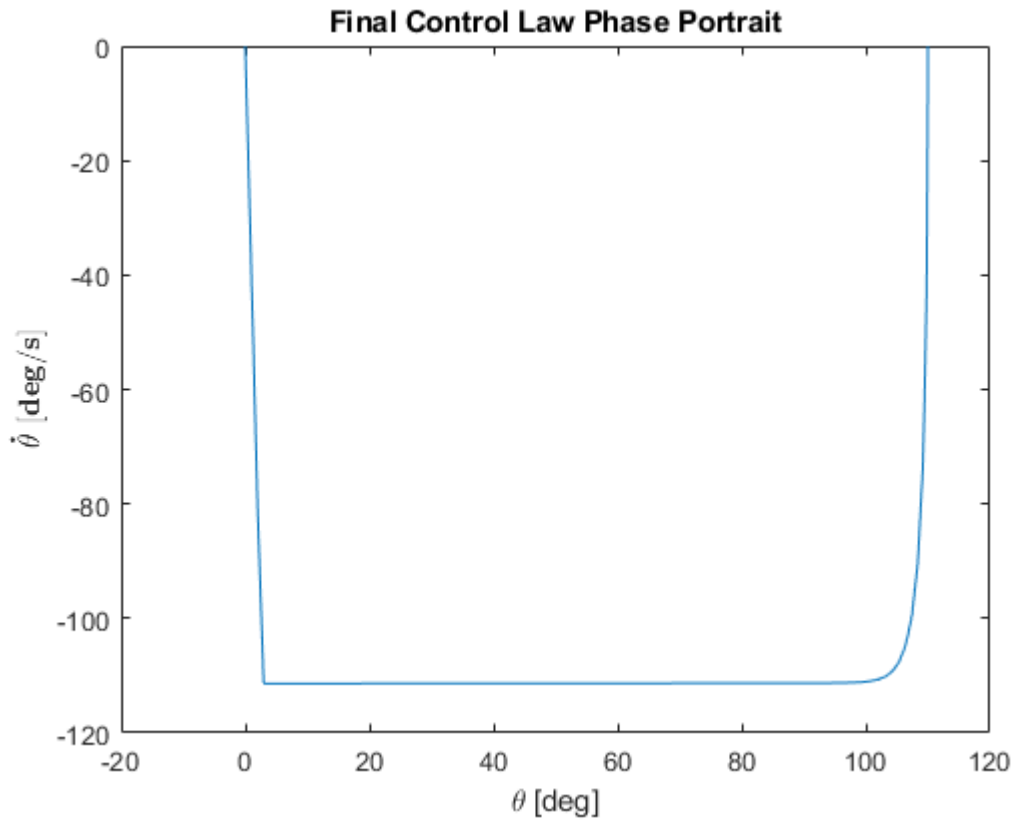$$\lambda = 45$$

$$C_{BL} = 1$$

The simulation is conducted in the same manner as before. Results are presented below.

Simulation 5

The final simulation uses the finalized control parameters.

Final Control Law Simulation

A phase portrait is also presented for comparison with experimental results.

Final Control Law Phase Portrait

This control response satisfies the design requirements and will be submitted for hardware testing. The performance of the finalized control law is tabulated below.

$$\theta_{ss} \approx -4.6 * 10^{-4} \ [deg]$$

$$t_{ss} \approx 1.3 \ [s]$$

$$|\hat{v}| \ << \ 15 \ [V]$$

No Actuation Chatter

Robustness Supported With Lyapunov Argument

The performance is achieved under ideal conditions as the nullifying voltage was derived from the same model used in the simulation. Despite this, the control law should hold up well to model uncertainty and final performance metrics are predicted to be similar.